NOAA Technical Report NOS CO-OPS 083

GLOBAL AND REGIONAL SEA LEVEL RISE SCENARIOS FOR THE UNITED STATES

Photo: Ocean City, Maryland

Silver Spring, Maryland
January 2017

noaa National Oceanic and Atmospheric Administration

U.S. DEPARTMENT OF COMMERCE
National Ocean Service
Center for Operational Oceanographic Products and Services

Center for Operational Oceanographic Products and Services
National Ocean Service
National Oceanic and Atmospheric Administration
U.S. Department of Commerce

The National Ocean Service (NOS) Center for Operational Oceanographic Products and Services (CO-OPS) provides the National infrastructure, science, and technical expertise to collect and distribute observations and predictions of water levels and currents to ensure safe, efficient and environmentally sound maritime commerce. The Center provides the set of water level and tidal current products required to support NOS' Strategic Plan mission requirements, and to assist in providing operational oceanographic data/products required by NOAA's other Strategic Plan themes. For example, CO-OPS provides data and products required by the National Weather Service to meet its flood and tsunami warning responsibilities. The Center manages the National Water Level Observation Network (NWLON), a national network of Physical Oceanographic Real-Time Systems (PORTS®) in major U. S. harbors, and the National Current Observation Program consisting of current surveys in near shore and coastal areas utilizing bottom mounted platforms, subsurface buoys, horizontal sensors and quick response real time buoys. The Center: establishes standards for the collection and processing of water level and current data; collects and documents user requirements, which serve as the foundation for all resulting program activities; designs new and/or improved oceanographic observing systems; designs software to improve CO-OPS' data processing capabilities; maintains and operates oceanographic observing systems; performs operational data analysis/quality control; and produces/disseminates oceanographic products.

Global and Regional Sea Level Rise Scenarios for the United States

William V. Sweet
National Oceanic and Atmospheric Administration, Center for Operational Oceanographic Products and Services, Silver Spring, MD, USA

Robert E. Kopp
Department of Earth & Planetary Sciences, Rutgers Energy Institute and Institute of Earth, Ocean & Atmospheric Sciences, Rutgers University–New Brunswick, New Brunswick, NJ, USA

Christopher P. Weaver
U.S. Environmental Protection Agency, Office of Research and Development, Research Triangle Park, NC, USA

Jayantha Obeysekera
South Florida Water Management District, West Palm Beach, FL

Radley M. Horton
Center for Climate Systems Research, Columbia University Earth Institute, New York, NY, USA

E. Robert Thieler
U.S. Geological Survey, Woods Hole, MA, USA

Chris Zervas
National Oceanic and Atmospheric Administration, Center for Operational Oceanographic Products and Services, Silver Spring, MD, USA

January 2017

RUTGERS
UNIVERSITY | NEW BRUNSWICK

U.S. DEPARTMENT OF COMMERCE
Penny Pritzker, Secretary

National Oceanic and Atmospheric Administration
Dr. Kathryn Sullivan, NOAA Administrator and Under Secretary of Commerce for Oceans and Atmosphere

National Ocean Service
Dr. Russell Callender, Assistant Administrator

Center for Operational Oceanographic Products and Services
Richard Edwing, Director

NOTICE

Mention of a commercial company or product does not constitute an endorsement by NOAA. Use of information from this publication for publicity or advertising purposes concerning proprietary products or the tests of such products is not authorized.

TABLE OF CONTENTS

LIST OF FIGURES

LIST OF TABLES

EXECUTIVE SUMMARY

The Sea Level Rise and Coastal Flood Hazard Scenarios and Tools Interagency Task Force, jointly convened by the U.S. Global Change Research Program (USGCRP) and the National Ocean Council (NOC), began its work in August 2015. The Task Force has focused its efforts on three primary tasks: 1) updating scenarios of global mean sea level (GMSL) rise, 2) integrating the global scenarios with regional factors contributing to sea level change for the entire U.S. coastline, and 3) incorporating these regionally appropriate scenarios within coastal risk management tools and capabilities deployed by individual agencies in support of the needs of specific stakeholder groups and user communities. This technical report focuses on the first two of these tasks and reports on the production of gridded relative sea level (RSL, which includes both ocean-level change and vertical land motion) projections for the United States associated with an updated set of GMSL scenarios. In addition to supporting the longer-term Task Force effort, this new product will be an important input into the USGCRP Sustained Assessment process and upcoming Fourth National Climate Assessment (NCA4) due in 2018. This report also serves as a key technical input into the in-progress USGCRP Climate Science Special Report (CSSR).

In order to bound the set of GMSL rise scenarios for year 2100, we assessed the most up-to-date scientific literature on scientifically supported upper-end GMSL projections, including recent observational and modeling literature related to the potential for rapid ice melt in Greenland and Antarctica. The projections and results presented in several peer-reviewed publications provide evidence to support a physically plausible GMSL rise in the range of 2.0 meters (m) to 2.7 m, and recent results regarding Antarctic ice-sheet instability indicate that such outcomes may be more likely than previously thought. To ensure consistency with these recent updates to the peer-reviewed scientific literature, we recommend a revised 'extreme' upper-bound scenario for GMSL rise of 2.5 m by the year 2100, which is 0.5 m higher than the upper bound scenario from Parris et al. (2012) employed by the Third NCA (NCA3). In addition, after consideration of tide gauge and altimeter-based estimates of the rates of GMSL change over the past quarter-century and of recent modeling of future low-end projections of GMSL rise, we revise Parris et al. (2012)'s estimate of the lower bound upward by 0.1 m to 0.3 m by the year 2100.

This report articulates the linkages between scenario-based and probabilistic projections of future sea levels for coastal-risk planning, management of long-lived critical infrastructure, mission readiness, and other purposes. The probabilistic projections discussed in this report recognize the inherent dependency (conditionality) of future GMSL rise on future greenhouse-gas emissions and associated ocean-atmosphere warming. In recognition of the different time horizons of relevance to different decision contexts, as well as the long-term GMSL rise commitment (lagged GMSL response) from on-going increases in ocean-atmosphere warming, GMSL rise and associated RSL change are quantified from the year 2000 through the year 2200 (on a decadal basis to 2100 and with lower temporal frequency between 2100 and 2200).

The 0.3 m-2.5 m GMSL range for 2100 is discretized by 0.5-m increments and aligned with emissions-based, conditional probabilistic storylines and global model projections into six GMSL rise scenarios: a *Low*, *Intermediate-Low*, *Intermediate*, *Intermediate-High*, *High* and *Extreme*, which correspond to GMSL rise of 0.3 m, 0.5 m, 1.0 m, 1.5 m, 2.0 m and 2.5 m, respectively. These GMSL rise scenarios are used to derive regional RSL responses on a 1-degree grid covering the coastlines of the U.S. mainland, Alaska, Hawaii, the Caribbean, and the Pacific island territories, as well as at the precise locations of tide gauges along these coastlines. These scenario-based RSL values fill a major gap in climate information needed to

support a wide range of assessment, planning, and decision-making processes. GMSL was adjusted to account for key factors important at regional scales, including: 1) shifts in oceanographic factors such as circulation patterns; 2) changes in the Earth's gravitational field and rotation, and the flexure of the crust and upper mantle, due to melting of land-based ice; and 3) vertical land movement (VLM; subsidence or uplift) due to glacial isostatic adjustment (GIA, which also changes Earth's gravitational field and rotation, as well as the overall shape of the ocean basin), sediment compaction, groundwater and fossil fuel withdrawals, and other nonclimatic factors. Key findings include:

- Along regions of the Northeast Atlantic (Virginia coast and northward) and the western Gulf of Mexico coasts, RSL rise is projected to be greater than the global average for almost all future GMSL rise scenarios (e.g., 0.3-0.5 m or more RSL rise by the year 2100 than GMSL rise under the Intermediate scenario).
- Along much of the Pacific Northwest and Alaska coasts, RSL is projected to be less than the global average under the Low-to-Intermediate scenarios (e.g., 0.1-1 m or less RSL rise by the year 2100 than GMSL rise under the Intermediate scenario).
- Along almost all U.S. coasts outside Alaska, RSL is projected to be higher than the global average under the Intermediate-High, High and Extreme scenarios (e.g., 0.3-1 m or more RSL rise by the year 2100 than GMSL rise under the High scenario).

Finally, the consequences of rising RSL are presented in terms of how the frequency of moderate-level flooding associated with a NOAA coastal/lakeshore flood *warning* of a serious risk to life and property may change in the future under the sea level scenarios. The elevation threshold used to classify such events by NOAA on their tide gauges varies along the U.S. coastline, but in general it is about 0.8 m (2.6 feet) above the highest average tide and locally has a 20% annual chance of occurrence. For example, using the flood-frequency definition, we find at most locations examined (90 cities along the U.S. coastline outside of Alaska) that with only about 0.35 m (<14 inches) of local RSL rise, annual frequencies of such disruptive/damaging flooding will increase 25-fold by or about (±5 years) 2080, 2060, 2040 and 2030 under the Low, Intermediate-Low, Intermediate and Intermediate High subset of scenarios, respectively.

1.0 INTRODUCTION

Long-term sea level rise driven by global climate change presents clear and highly consequential risks to the United States over the coming decades and centuries. Today, millions of people in the United States already live in areas at risk of coastal flooding, with more moving to the coasts every year (Melillo et al., 2014). Rising seas will dramatically increase the vulnerability of this growing population, along with critical infrastructure related to transportation, energy, trade, military readiness, and coastal ecosystems and the supporting services they provide (Parris et al., 2012; Hall et al., 2016). One recent study estimates that 0.9 meters (m) of sea level rise would permanently inundate areas currently home to 2 million Americans; 1.8 meters would inundate areas currently home to 6 million Americans (Hauer et al., 2016).

Global mean sea level (GMSL) has increased by about 21 centimeters (cm) to 24 cm (8–9 inches [in]) since 1880, with about 8 cm (3 in) occurring since 1993 (Church and White, 2011; Hay et al., 2015; Nerem et al., 2010). In addition, the rate of GMSL rise since 1900 has been faster than during any comparable period over at least the last 2800 years (Kopp et al., 2016a). As is discussed in detail in this report, scientists expect that GMSL will continue to rise throughout the 21st century and beyond, because of global warming that has already occurred and warming that is yet to occur due to the still-uncertain level of future emissions. GMSL rise is a certain impact of climate change; the questions are *when*, and *how much*, rather than *if*. There is also a long-term commitment (persistent trend); even if society sharply reduces emissions in the coming decades, sea level will most likely continue to rise for centuries (Golledge et al., 2015; DeConto and Pollard, 2016).

While the long-term, upward shift in sea level is an underlying driver of changes to the nation's coasts, impacts are generally expressed through extreme water levels (short-period, lower-probability events both chronic and acute in nature) occurring against the background of this shifting baseline. Higher sea levels worsen the impacts of storm surge, high tides, and wave action (e.g., Theuerkauf et al., 2014), even absent any changes in storm frequency and intensity. Even the relatively small increases in sea level over the last several decades have led to greater storm impacts at many places along the U.S. coast (Parris et al., 2012; Miller et al., 2013; Sweet et al., 2013). Similarly, the frequency of intermittent flooding associated with unusually high tides has increased rapidly (accelerating in many locations) in response to increases in relative sea level (RSL) as shown in Figure 1. At some locations in the United States, the frequency of tidal flooding (events typically without a local storm present) has increased by an order of magnitude over the past several decades, turning it from a rare event into a recurrent and disruptive problem (Sweet et al., 2014; Sweet and Park, 2014; Sweet et al., 2016). Significant, direct impacts of long-term RSL rise, including loss of life, damage to infrastructure and the built environment, permanent loss of land (Weiss et al., 2011), ecological regime shifts in coastal wetlands and estuary systems (Kirwan et al., 2010), and water quality impairment (Masterson et al., 2014), also occur when key thresholds in the coastal environment are crossed (Wong et al., 2014). Some of these impacts have the potential to 'feedback' and influence wave impacts and coastal flooding. For example, there is evidence that wave action and flooding of beaches and marshes can induce changes in coastal geomorphology, such as sediment build up, that may iteratively modify the future flood risk profile of communities and ecosystems (Lentz et al., 2016).

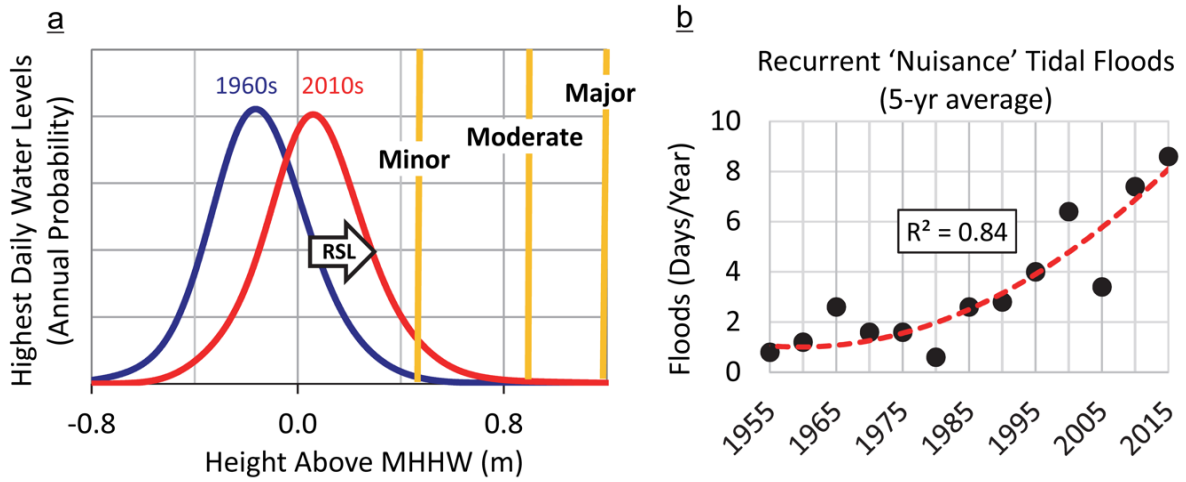

Figure 1. a) Multi-year empirical (smoothed) distributions for daily highest water levels in Norfolk, Va. (Sweet and Park 2014) for the 1960s and 2010s, showing extent that local RSL rise has increased the flood probability relative to impact thresholds defined locally by the National Weather Service (http://water.weather.gov/ahps) for minor (~0.5 m: *nuisance* level), moderate (~0.9 m) and major (~1.2 m: local level of Hurricane Sandy in 2012) impacts, relative to mean higher high water (MHHW) tidal datum of the National Tidal Datum Epoch (1983–2001). b) Due to RSL rise, annual flood frequencies (based upon 5-year averages) in Norfolk for recurrent nuisance tidal floods with minor impacts are accelerating, as shown by the quadratic trend fit (goodness of fit [R^2]=0.84). Flood rates are rapidly increasing in similar fashions along dozens of coastal cities of the U.S. (e.g., Sweet et al., 2014; Sweet and Park, 2014; Sweet and Marra, 2016).

In this context, there is a clear need—and a clear call from states and coastal communities (White House, 2014)—to support preparedness planning with consistent, accessible, authoritative and more locally appropriate knowledge, data, information, and tools about future changes in sea level and associated coastal risks. In response to this need, the White House Council on Climate Preparedness and Resilience in 2015 called for the establishment of the Federal Interagency Sea Level Rise and Coastal Flood Hazard Scenarios and Tools Task Force,[1] a joint task force of the National Ocean Council (NOC) and the U.S. Global Change Research Program (USGCRP). The Task Force's charge is to develop and disseminate, through interagency coordination and collaboration, future RSL and associated coastal flood hazard scenarios and tools for the entire United States. These scenarios and tools are intended to serve as a starting point for on-the-ground coastal preparedness planning and risk management processes, including compliance with the new Federal Flood Risk Management Standard (FFRMS).[2] The Task Force is charged with leveraging the best available science; incorporating regional science and expertise where appropriate; building this information into user-friendly mapping, visualization, and analysis tools; and making it easily accessible through established Federal web portals.[3] Part of the motivation for forming the Task Force was to bring together key efforts within individual agencies, such as the Federal Emergency Management Agency (FEMA), National Oceanic and Atmospheric Administration (NOAA), U.S. Army Corps of Engineers (USACE), U.S. Geological Survey (USGS), Department of Defense (DoD), Environmental Protection Agency (EPA) and National Aeronautics and Space Administration (NASA), that could serve as building blocks of an overall Federal system of sea level information and decision support, and to provide synthesis and coverage of the entire United States coastline.

---

[1] See appendix A for Task Force membership.

[2] E.O. 13690: Establishing a Federal Flood Risk Management Standard and a Process for Further Soliciting and Considering Stakeholder Input (https://www.whitehouse.gov/the-press-office/2015/01/30/executive-order-establishing-federal-flood-risk-management-standard-and-)

[3] e.g., Digital Coast, globalchange.gov, and the Climate Resilience Toolkit

This report describes the output from a set of subtasks of the overall Task Force effort—specifically, developing updated scenarios of GMSL rise, and then regionalizing these global scenarios for the entire U.S. coastline, to serve as inputs into assessments of potential vulnerabilities and risks in the coastal environment. In addition to supporting the longer-term Task Force goals, this new set of products will also be a key input into the USGCRP Sustained Assessment process and the upcoming Fourth National Climate Assessment (NCA4), due in 2018, including serving as a technical input to the in-progress USGCRP Climate Science Special Report (CSSR).

This current effort builds upon recent advances in both sea level science and the synthesis and assessment of this science to support planning and decision-making needs. A Federal interagency effort described in Parris et al. (2012) defined a set of future GMSL rise scenarios that spanned the range of published estimates (at the time of development of the report), and could be used to support assessment and planning. The two-fold purpose of Parris et al. (2012) was to provide a scientific synthesis across the large range of published future GMSL rise estimates and to complement existing scientific assessments (e.g., from the Intergovernmental Panel on Climate Change [IPCC]) by presenting the science from the perspective of scenario analysis within a risk-based context. The report noted the wide range of estimates for GMSL rise scattered throughout the scientific literature, along with the lack of any coordinated, interagency effort in the United States to harness this literature in the development of agreed-upon estimates to support coastal planning, policy, and management. Coastal managers had correspondingly been left to identify appropriate and relevant scenarios on an *ad hoc* basis. Parris et al. (2012) developed a set of four scenarios, spanning a range of 0.2 to 2.0 m by the year 2100, that described potential future GMSL conditions under varying assumptions about climate change and the behavior of large ice sheets.

The four Parris et al. (2012) GMSL rise scenarios were designed to help planning, policy, and decision-making stakeholders analyze vulnerabilities and future risks under conditions of scientific uncertainty. As discussed in more detail below, a key advance of Parris et al. (2012) was to evaluate the available science from the perspective of user needs, expanding the range of future conditions considered to support a diversity of users with potentially very different decision contexts and risk tolerances in their planning. This includes the need to test plans and policies against extreme cases with a low probability of occurrence but severe consequences if realized. The Parris et al. scenarios initially served as input into the Third NCA (NCA3; Melillo et al., 2014), but have since been taken up in a variety of assessment, planning, and decision-making processes at the Federal, state, and local level (e.g., USACE, 2014), illustrating the clear demand for such information, even when available only for GMSL.

Although Parris et al. (2012) represented a significant step forward in developing actionable ranges of sea level rise and placing them in an applied context, it had several limitations that subsequent efforts have sought to address. For example, planners would greatly benefit from more locally and regionally relevant information that accounts for location-specific adjustments to GMSL. In addition, sea level science has advanced significantly over the last few years, especially improving understanding of the complex behaviors of the large, land-based ice sheets in Greenland and Antarctica under global warming, and the correspondingly larger range of possible 21st century rise in GMSL than previously thought (Oppenheimer and Alley, 2016; DeConto and Pollard, 2016). Two recent efforts representing significant progress in providing updated future GMSL and RSL rise information are the U.S. DoD Coastal Assessment Regional Scenario Working Group study, reported in Hall et al. (2016), and Kopp et al. (2014). Both produced local-scale RSL rise estimates across a range of future GMSL rise values: at individual U.S. military installations worldwide in Hall et al. (2016) and for a global network of tide

gauge locations in Kopp et al. (2014). Hall et al. (2016) used the Parris et al. (2012) GMSL rise scenarios as the basis for their regional adjustments, while Kopp et al. (2014) constructed probabilistic projections of the factors driving GMSL rise as the basis for their estimates of the probability of different levels of relative sea level change (conditional on alternative scenarios of greenhouse gas emissions) at a global tide gauge network. Since the analysis described in this report draws extensively from both studies, the approach, findings, and underlying methodology of both are discussed in more detail in the following sections.

These two efforts provide the foundation for the current development of regional gridded RSL scenarios for the United States. This report leverages this prior work to generate a new set of sea level products that represents 1) the most up-to-date science and 2) the most up-to-date set of methodologies for regionally adjusting a given GMSL rise scenario. In addition, it attempts to better support both scientific assessment and decision-making by providing a more unified look across both emissions-dependent probabilistic approaches and discrete scenario-based methods, as conceptualized in Figure 2.

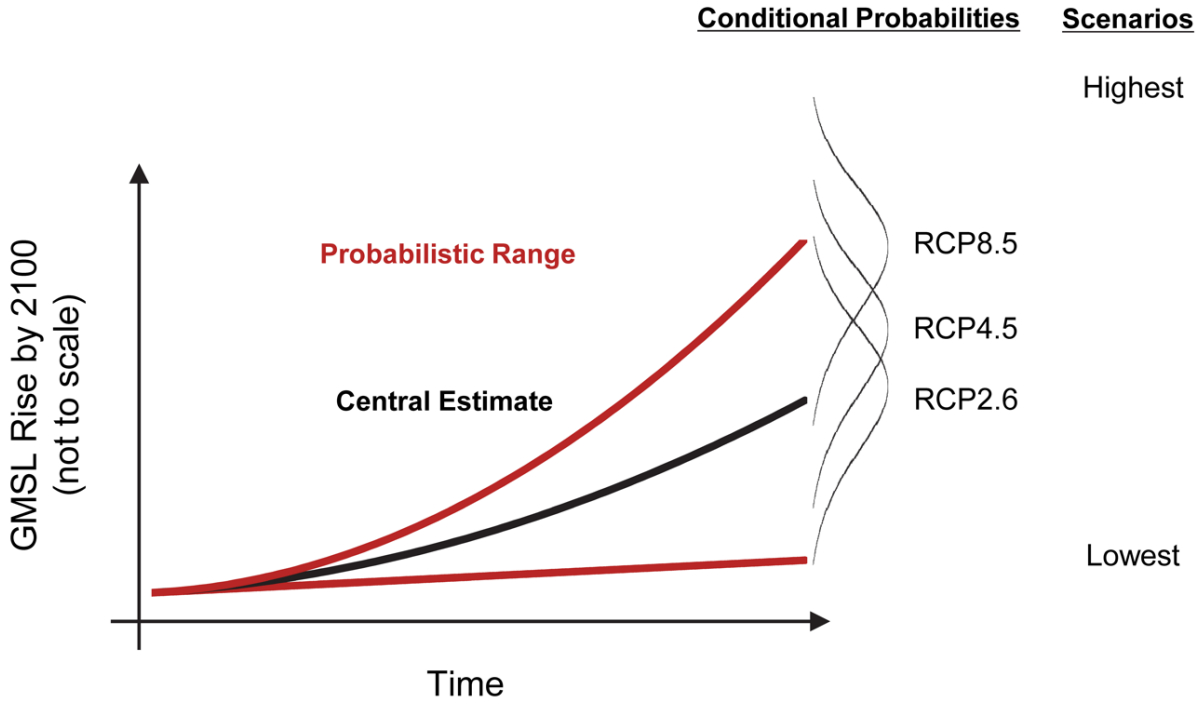

Figure 2. Schematic showing the intersection of scenario approaches with emission-dependent (conditional) probabilistic projections of sea level rise under the climate modeling community's Representative Concentration Pathways (RCP) (van Vuuren et al., 2011).

This report pursues the development of new sea level scenario products from a risk-based perspective, where the primary motivation is to synthesize the available science and identify appropriate scenarios to support evaluation and management of future risks associated with rising seas. As described in Hinkel et al. (2015), the goals of traditional scientific assessment can often diverge from the goals of packaging science needed to support assessment and management of risk. For example, the IPCC Fifth Assessment Report (AR5; Church et al., 2013a) stresses the central or 'likely' range of 21st century rise in GMSL based primarily on process-based models. As defined by the IPCC, the 'likely' range is assessed as having at least a 66% probability of containing the true value; as Church, et al. (2013b) explained, the chapter authors assessed that "there [was] roughly a one-third probability that sea level

rise by 2100 may lie outside the 'likely' range." Risk-averse decision-makers, however, may find the IPCC's 'likely' range of future GMSL rise inadequate for their planning purposes, given the roughly 33% chance that GMSL rise falls outside of this range. For example, the operator and regulator of a nuclear power plant near the coastal zone might be more interested in the 99th percentile (or 99.9th percentile, etc.) of the estimated future distribution of GMSL outcomes to robustly manage their risks, since a disproportionate fraction of total risk will often be associated with low-probability (but high-consequence) outcomes; many impacts in the coastal environment are highly nonlinear with respect to the amount of RSL rise (Gutierrez et al., 2009). For example, in the Thames Estuary 2100 project, planners considered a plausible worst-case RSL rise scenario as a key part of the technical analysis developed in support of planning new flood-control infrastructure to protect the city of London from tidal flooding of the Thames River basin over the 21st century (Ranger et al., 2013). Such a risk-based approach, with consideration of the full range of scientifically plausible outcomes including potentially consequential outcomes with low probability of occurrence, is consistent with standard practice in a variety of risk-centered fields, from insurance to environmental toxicology. In very general terms, synthesis and assessment of the best-available science to most effectively support risk assessment should not only aim to address the question, "What is most likely to occur?" but also "How bad could things get?" along with other questions relevant to the current state of knowledge, rate of change, time of emergence of extreme impacts, when more might be known, and so on.

Accordingly, this report assesses global and regional sea level rise science pertinent to assessing U.S. coastal risks, including how best to characterize uncertainty to support planning and decision-making in a consistent manner nationwide. This kind of bounding analysis is often given much less attention in traditional climate science assessments, so this report focuses more substantially on it with respect to future sea levels along U.S. coasts.

Therefore, in support of these goals, the focus in this report is on:

- Examining the full range of scientifically plausible future rises in sea level and leveraging multiple lines of scientific evidence, not just the process-based models that have important known deficiencies with respect to the representation of ice sheet dynamics (sections 2-5)
- Providing scenario selection guidelines for planning and decision-making applications as a function of decision context (section 6)

Sections 2-5 are therefore primarily scientific and technical, describing the observational record, the foundational work upon which this current effort is built, and the results of the analysis, whereas Section 6 is geared more toward the needs of users for applying these results in planning processes. Section 7 concludes the report by providing a summary and a look ahead.

2.0 SEA LEVEL RISE: HISTORIC INSIGHTS AND RECENT OBSERVATIONS

Updated estimates of possible future GMSL and RSL rise amounts and associated rates depend in part upon historical sea level rise. This section reviews recent observations of sea level change in the context of recent reconstructions of past responses.

Water levels vary in response to multiple processes operating over multiple temporal and spatial scales (Table 1; see Kopp et al. (2015) for a review). Changes in RSL occur in response to changing sea surface height (SSH) and due to both natural and anthropogenic VLM (where a downward sinking land motion with a 'negative' sign contributes to a RSL rise) and can be expressed as:

$$1)\quad \Delta RSL = \Delta SSH - VLM$$

In a simple view, long-term trends in global SSH arise from increases in global ocean volume (due primarily thermal expansion) and ocean mass additions (due to primarily to melting of land-based ice, with changes in storage of water on land). Superimposed are several factors that can cause changes in regional SSH, including decadal-scale variability in ocean circulation (e.g., Firing et al., 2004), often associated with large-scale climatic patterns such as the Pacific Decadal Oscillation (PDO; Bromirski et al., 2011), as well as interannual variability such as occurs during phases of the El Niño Southern Oscillation (ENSO, Hamlington et al., 2015). RSL change also arises from regional and more-localized VLM. VLM can be downward (negative rates; i.e., subsidence) or upward (positive rates; i.e., uplift) and cause a relative rise or drop in sea levels, respectively. VLM results from natural processes (e.g., GIA or sediment compaction) whose rates are quasi-steady for centuries, as well as more punctuated natural events (e.g., earthquakes). Human-induced VLM is another contributor, typically associated with local-to-regional groundwater and fossil-fuel withdrawal that have time scales associated with the disturbance.

Table 1. Spatial and temporal scales of geophysical processes affecting water levels.

Physical Process	Spatial Scale			Temporal Scale	Potential Magnitude (yearly)
	Global	Regional	Local		
Wind Waves (e.g., dynamical effects, runup)			X	seconds to minutes	<10 m
Tsunami		X	X	minutes to hours	<10s of m
Storm Surge (e.g., tropical storms or nor'easters)		X	X	minutes to days	<15 m
Tides			X	hours	<15 m
Seasonal Cycles		X	X	months	<0.5 m
Ocean/Atmospheric Variability (e.g., ENSO response)		X	X	months to years	<0.5 m
Ocean Eddies, Planetary Waves		X	X	months to years	<0.5 m
Ocean Gyre and Over-turning Variability (e.g., PDO response)		X	X	years to decades	<0.5 m
Land Ice Melt/Discharge	X	X	X	years to centuries	millimeters to centimeters
Thermal Expansion	X	X	X	years to centuries	millimeters to centimeters
Vertical Land Motion		X	X	minutes to centuries	millimeters to centimeters

Changes in SSH are measured by satellite altimeters, which observe subtidal water levels offshore. Changes in nearly instantaneous water level (for safe navigation, storm-surge preparedness and other commerce-supporting activities) and in RSL (including VLM effects) are measured by tide gauges at the land-ocean interface. However, it should be noted that, in the discussion of the consequences of RSL rise on tidal flood frequencies (see section 6), waves and their high-frequency (seconds to minutes) dynamical effects are not considered; we refer to 'still water levels' instead of a more 'total water level' (Hall et al., 2016) as operationally reported by tide gauges due to the mechanical low-pass filtering associated with their protective wells, multi-minute averaging scheme and general placement in protected waters (Sweet et al., 2015). Also, for context, the term 'sea level' is distinguished from 'water level' in that the former is generally considered to represent monthly and longer-scale variability; when discussing spatial scales, responses locally refer loosely to scales upwards of about tens of kilometers and regionally to scales upwards of about hundreds of kilometers.

2.1 Global Mean Sea Level Changes

As shown in Figure 3a, the rate of GMSL rise as measured by altimeter (3.4 ± 0.4 mm/year) since 1993 (https://sealevel.nasa.gov; accessed in December, 2016) is more than double the rate estimated by a global network of tide gauges during the 20th century (~1.4 mm/year; Church and White, 2011; Hay et al., 2015), and the 20th century rate is found to be faster than any century in at least 2800 years (Kemp et al., 2011; Kopp et al., 2016a). The altimeter and tide gauge reconstructions of GMSL (Figure 3a) are in close agreement during their common record (since 1993). Over the last 30 years (since the mid 1980's), tide gauge based reconstructions of GMSL report trends of ~3 mm/year. The main drivers for GMSL rise are atmospheric and ocean warming, which act to increase both the mass of the ocean, primarily through the melting of land ice (anthropogenic changes in the storage of water on land has been an additional effect), and the volume of the ocean, primarily through thermal expansion. Over the last decade, these three components measured by satellite gravimetry measurements of GRACE (Gravity Recovery and Climate Experiment) (www.nasa.gov/grace) and in situ by the worldwide array of Argo profiling drifters (www.argo.ucsd.edu) explain the global altimeter trend (Leuliette, 2015; Merrifield et al., 2015; Chambers et al., 2016; Leuliette and Nerem, 2016) (Figure 3b).

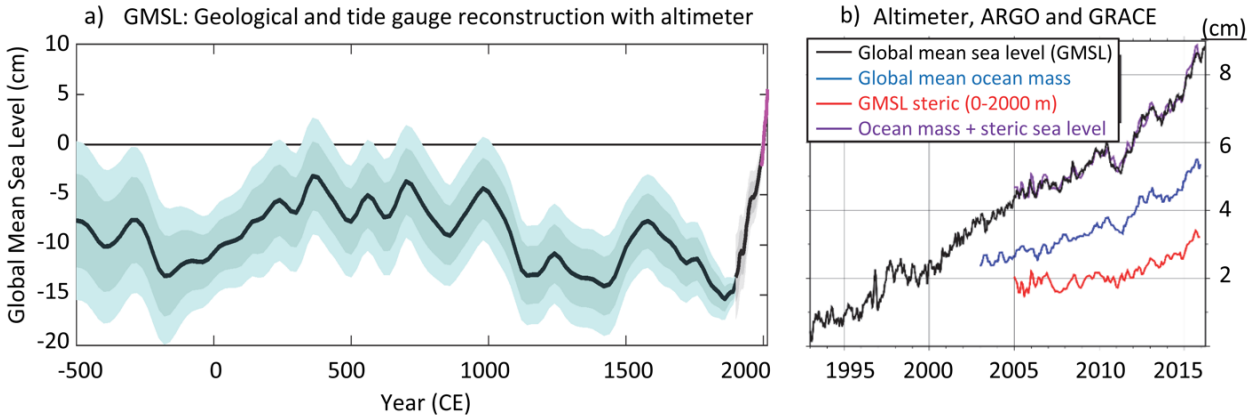

Figure 3. a) GMSL rise from -500 to 1900 CE from Kopp et al. (2016a)'s geological and tide gauge-based reconstruction [black line with blue error estimates], from 1900 to 2010 from Hay et al. (2015)'s tide gauge-based reconstruction [black], and from 1992 to 2015 from the satellite-based reconstruction updated from Nerem et al. (2010) [magenta] and b) comparisons of GMSL since 1992 from NOAA/NESDIS/STAR (black line) and the summation (purple line) of global mean ocean mass from GRACE (blue line) and steric (density) sea level from Argo (red line) with seasonal variations removed and 60-day smoothing applied (from Leuliette and Nerem, 2016).

2.2 Regional Sea Level Changes

Consistent with scientific understanding, sea levels have not been rising uniformly across the globe over the last century (Church et al., 2004; Hay et al., 2015; Merrifield et al., 2016) or indeed at any time for which geological records exist (Khan et al., 2015; Kopp et al., 2016a); sea level has been spatially quite variable (Figure 4a). One driver of differences is the dynamic redistribution of ocean mass, which is the result of both episodic and long-term changes in winds, air pressure, air-sea heat and freshwater fluxes, and ocean currents. There are two regional patterns that impact U.S. coastlines:

- There has been a large west-to-east difference in sea level rise rates across the Pacific Basin over the last several decades. Trends range from much higher than the global rate (>10 mm/year) within the Western Pacific and at several U.S. Affiliated Pacific Islands (USAPI) to much less (<1 mm/year) within the Eastern Pacific and regions of the U.S. West Coast (Figure 4a). These zonal rate differences are thought to be primarily associated with multi-decadal fluctuations in basin-scale forcing driven primarily by altered prevailing trade wind forcing associated with the PDO (Bromirski et al., 2011; Merrifield et al., 2012), which appears to have switched phases in the last couple of years (Hamlington et al., 2016; Merrifield et al., 2016). A PDO-phase switch could signal the start of higher amounts of RSL rise along the U.S. West Coast in the coming decades, similar to higher rates that have occurred there during portions of the last century (Zervas, 2009; Church et al., 2004).
- Along the Northeast Atlantic, sea level trends have been higher than the global rate over the last several decades, capped by a recent multiyear jump in sea level beginning in 2009 (Goddard et al. 2015). The relatively high rates have been attributed to changes in the Gulf Stream (Yin and Goddard, 2013; Ezer, 2013; Kopp, 2013; Kopp et al., 2015), although there is some debate as to whether these changes represent natural variability or a long-term trend (Rahmstorf et al., 2015).

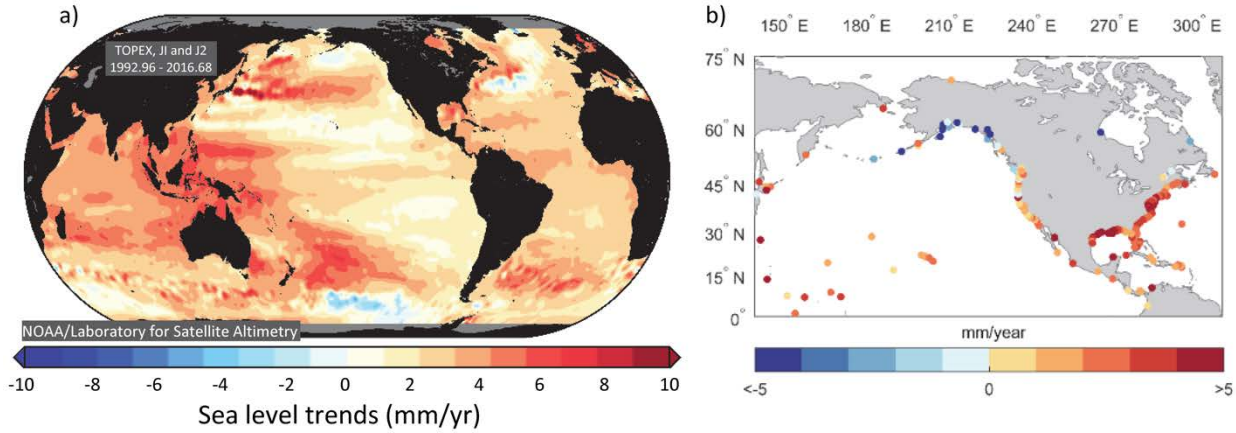

Figure 4. a) Sea level change rates from 1992-2016 from TOPEX/Poseidon, Jason-1 and Jason-2 (www.star.nesdis.noaa.gov/sod/lsa/SeaLevelRise) and b) relative sea level trends based upon full record (>30-year period of record in all cases) measured and published for NOAA tide gauges through 2015 (tidesandcurrents.noaa.gov/sltrends).

2.3 Relative Sea Levels

Around the U.S., VLM can be a significant factor in the overall rate of RSL trends experienced. As shown in Figure 4b, the highest RSL rise trends are found in regions of Louisiana (8–10 mm/year), Texas (4–7 mm/year) and along the Northeast Atlantic from Virginia to New Jersey (3–5 mm/year). In these regions, natural, nonclimatic processes like GIA and sediment compaction add about 0.5–

2 mm/year to RSL change (Kopp et al., 2016a), while artificial groundwater and oil/gas extraction processes further enhance RSL rise (Galloway et al., 1999; Sella et al., 2007; Boon et al., 2010; Eggleston and Pope, 2013; Miller et al., 2013). Where RSL-rise trends are high, land subsidence with rates of 2–5 mm/year or more is not uncommon as estimated by global positioning systems (GPS) for regions of the Northeast Atlantic and Gulf Coasts (Figure 5). On the other hand, there are regions, such as parts of southern Alaska, where RSL trends are negative with land uplift >10 mm/year. In Alaska, this is due to GIA-related uplift from the last ice age, as well as more recent uplift due to glacier retreat over the last several decades (e.g., Sato et al., 2011) and the averaged effects of tectonics over the observational record.

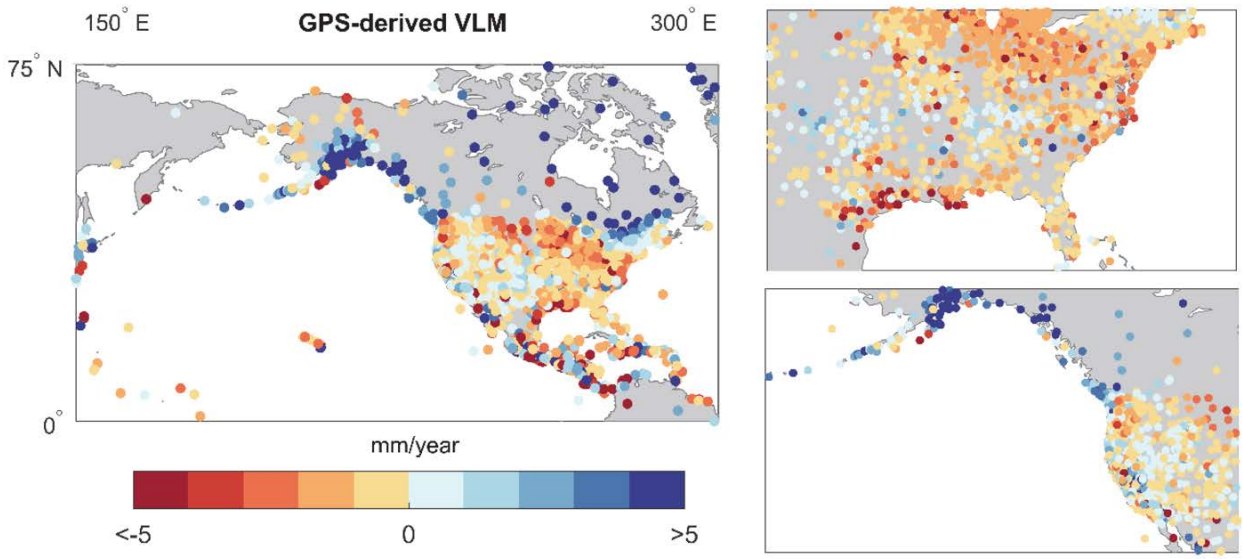

Figure 5. VLM trend estimates (mm/year) derived from GPS platforms used by Hall et al. (2016) obtained from NASA Jet Propulsion Laboratory (http://sideshow.jpl.nasa.gov/post/series.html accessed March 2016) and University of Wisconsin (personal communication March 2016, Chuck DeMets of the University of Wisconsin). The higher-resolution plots (on right) of the U.S. East and West/Alaskan Coast share the same color scale. Negative values (red colored) occur where VLM is downward, which increases RSL at the coast.

3.0 FUTURE SEA LEVELS: SCENARIOS AND PROBABILISTIC PROJECTIONS

As discussed in Kopp et al. (2014) and Hall et al. (2016), development of the scenario products reported on here starts with estimates of the probability of GMSL change and underlying contributing processes, conditional upon greenhouse-gas emissions pathways. These emissions pathways are represented by the Representative Concentration Pathways (RCPs) (van Vuuren et al., 2011). From these conditional probability distributions, scenarios to support planning and decision-making in the face of uncertain future sea level rise risks can be defined and selected, depending on the unique characteristics of a given decision, as will be discussed in more detail in section 6.

Because of the importance of sea level in a coastal-hazards context, and in light of these substantial global and regional trends, the natural question is how much GMSL might rise over the next few decades, this century, and beyond. Until recently, it has been commonplace for studies to provide a single 'mid-range' or 'central' projection (Tebaldi et al., 2012; NRC, 2012). Such an approach may be sufficient to address near-term planning needs, because at these timescales, variations in projected sea level rise—e.g., under current assumptions about future greenhouse gas emissions—will be small relative to the noise associated with storm surge activity. Such planning decisions could include normal budgeting cycles for anticipated high-water occurrences for preparedness purposes (e.g., budgeting for mobilization of personnel, pumps, sandbags and other temporary flood-control measures). However, mid-range projections are typically insufficient for many decisions. As discussed in section 1, decision-makers charged with planning for upgrades to existing long-life critical infrastructure (e.g., power plants, military installations), or building new infrastructure, need to consider the risks across a broad range of possible outcomes, including those associated with high-consequence, low-probability situations.

Parris et al. (2012) recognized the need for an interagency effort to define a set of future-possible GMSL rise scenarios for coastal planning, policy, and management to allow for recognition of trend changes and adaptive management strategies (USACE, 2013). Because of the large uncertainties involved in predictions of the land-based ice melt contribution to GMSL rise and the significant consequences associated with impossible-to-rule-out extreme outcomes, Parris et al. (2012) recommended a scenario approach covering a broad range (0.2 m to 2.0 m GMSL rise by 2100) of existing sea level study results (trends, process modeling, semi-empirical approaches, etc.). Their scenario set, which was developed to support NCA3 (Melillo et al., 2014), was not intended to provide probabilistic prediction of future changes. Rather, the scenarios were intended to describe plausible conditions that support decision-making under uncertainty, given specific assumptions about which sea level rise science to include in one's risk assessment. Parris et al. (2012) explicitly conceptualized scenarios as being defined by considerations of use, writing, *"Scenarios do not predict future changes, but describe future potential conditions in a manner that supports decision-making under conditions of uncertainty. Scenarios are used to develop and test decisions under a variety of plausible futures. This approach strengthens an organization's ability to recognize, adapt to, and take advantage of changes over time"* (Parris et al., 2012).

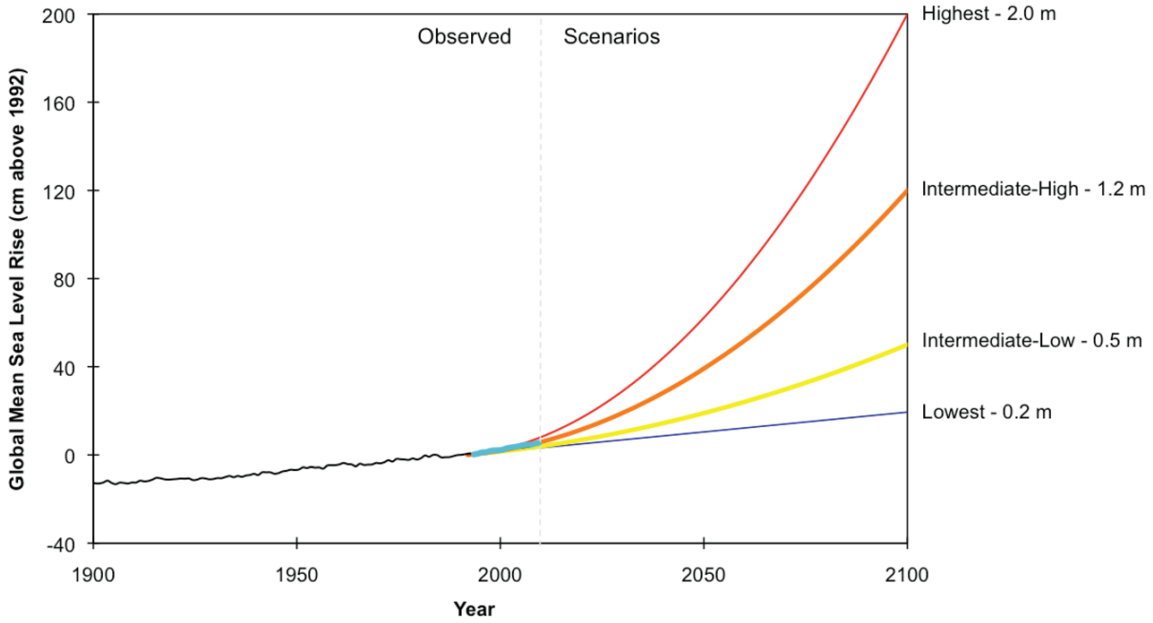

Figure 6. The GMSL rise scenarios of Parris et al. (2012).

The Parris et al. (2012) scenarios provided a range of possible future GMSL rise by 2100, bounded by a low- (0.2 m) and a high-end (2.0 m) member with two intermediate members (0.5 m and 1.2 m) (Figure 6). Each of these four scenarios exemplifies a specific set of scientific assumptions about 21st century GMSL. For example, the low scenario represents an amount about 5 cm above the extrapolated rate of the GMSL rise trend over the 20th century, while the high scenario represents an upper limit reflecting GMSL rise occurring under more extreme land-ice contributions, as modeled by Pfeffer et al. (2008). The two intermediate scenarios represent rise obtained from the upper-end of the projections from the IPCC Fourth Assessment Report, from climate models using the low-emissions B1 scenario (Intermediate-Low), and several semi-empirical based studies (Rahmstorf et al., 2007; Horton et al., 2008; Intermediate-High), respectively.

More recently, Hall et al. (2016) provided a set of five GMSL rise scenarios for 2100 (0.2, 0.5, 1.0, 1.5 and 2 m) with a similar, user-focused conceptual framing as Parris et al. (2012), including lower and upper bounds to provide a plausible range of GMSL-rise related risk of concern for DoD installation managers. Hall et al. (2016) assessed this GMSL range against the extant scientific literature after the Parris et al. (2012) report (discussed in the next section). Intermediate scenarios were simply discretized by 0.5-m increments and aligned with emissions-based, conditional probabilistic storylines and global model projections. In a significant update to Parris et al. (2012), Hall et al. (2016) also provided local adjustments to the global scenarios to provide site-specific scenarios, which are further described in section 4.

3.1 Probabilistic GMSL Rise Projections

Since the Parris et al. (2012) report, there have also been significant advances in developing probabilistic estimates of future GMSL. Estimates of full probability distributions of possible future GMSL outcomes (conditional on major assumptions such as future greenhouse gas emissions) provide decision-makers with the most comprehensive information base, from which they can select the most relevant individual scenarios to be used in their planning processes (Oppenheimer and Alley, 2016). Specifically, several recent studies have provided probabilistic projections of the extent of future

GMSL rise conditional on forcing from the RCPs (van Vuuren et al., 2011). The RCPs provide a set of possible future greenhouse gas concentrations through the year 2300 and were used by the IPCC AR5. Each RCP represents possible underlying (though implicit) socioeconomic conditions and technological considerations, including a low-end member (RCP2.6) requiring strong mitigation (net-negative emissions in the last decades of the 21st century), a moderate mitigation member (RCP4.5) stabilizing emissions through 2050 and declining thereafter, and a high-end, fossil-fuel-intensive, 'business-as-usual' emission scenario (RCP8.5). In response, global mean temperatures are modeled as likely (>66% probability) to increase 1.9–2.3, 2.0–3.6 and 3.2–5.4 degrees Celsius, respectively, for RCP2.6, RCP4.5 and RCP8.5 over the 2081–2100 period relative to 1850–1900 levels (IPCC, 2013).

The IPCC AR5 (Church et al., 2013a), using an ensemble of process-based models and other sources of information, projects a median and likely (66% probability) GMSL rise of 0.44 m (0.28–0.61 m), 0.53 m (0.36–0.71 m) and 0.74 m (0.52–0.98 m) by 2100 for RCP2.6, 4.5 and 8.5, respectively. (There is an additional pathway, RCP6.0, which is not analyzed here since its 21st-century GMSL projections are nearly identical to those for RCP4.5, and few models ran RCP6.0 projections beyond 2100.) However, AR5 recognized the challenges of modeling additions due to the collapse of marine-based sectors of the Antarctic ice sheet. More recent studies of GMSL rise have reported probability ranges that have focused on resolving ranges spanning lower probabilities and/or providing complete conditional probability distributions. An assessment of recent probabilistic studies finds GMSL rise by 2100 projected for the 90% probability (5th–95th%) range to fall between 0.25–0.80 m, 0.35–0.95 m and 0.5–1.3 m, respectively, for RCP2.6, 4.5 and 8.5 (Miller et al., 2013; Kopp et al., 2014, 2016a; Slangen et al., 2014; Mengel et al., 2016). These projections are consistent with the global temperature/GMSL relationship found to occur over the last 2800 years (Kopp et al., 2016a). To obtain GMSL rise estimates whose ranges extend beyond AR5, additional assumptions are included within a particular probabilistic framework. A few examples include reliance on structured expert elicitation of potential ice-melt contributions not captured in the process models (Bamber and Aspinall, 2013) or from geologic evidence comparing past sea levels and atmospheric greenhouse gas concentrations (Rohling et al., 2013) or temperature (Kopp et al., 2016a). Under such frameworks, estimates of high-end GMSL rise by 2100 under RCP8.5 include ~1.8 m [95th percentile] (Jevrejeva et al., 2014, Rohling et al., 2013 and Grinsted et al., 2015), ~2.2 m [99th percentile] (Jackson and Jevrejeva, 2016), and ~2.5 m [99.9th percentile] (Kopp et al., 2014).

3.2 Upper and Lower GMSL Rise Scenario Bounds

Determining a potential upper limit of GMSL rise by 2100 (and beyond) is considered an important target for critical and long-lived infrastructure decisions and a primary objective of this report. Since the upper limit established by Pfeffer et al. (2008), which was based primarily on assessment of the maximum plausible loss rate from Greenland and which was the basis for the 2.0-m high scenario for 2100 of Parris et al. (2012), there has been continued and growing evidence that both Antarctica and Greenland are losing mass at an accelerated rate based upon gravimetry satellites (GRACE), repeat altimetry, in-situ GPS monitoring, and input-output calculations (Shepherd et al., 2012; Khan et al., 2014; Scambos and Shuman, 2016; Seo et al., 2015; Martín-Español et al., 2016). Such evidence suggests that the collapse of some sectors of the Antarctic ice sheet may be inevitable as surrounding ocean waters warm (Joughin et al., 2014; Rignot et al., 2014). In addition, recent modeling of physical feedbacks related to marine ice-cliff instabilities and ice-shelf hydrofracturing (rain and meltwater-enhanced crevassing and calving) used within the physical process models generating GMSL estimates are being incorporated into ice-sheet models (Pollard et al., 2015). With such feedbacks modeled for Antarctica, additional GMSL rise upwards of 0.6–1.1 m to median estimates under RCP8.5 are possible

by 2100 (DeConto and Pollard, 2016), potentially raising median GMSL projections for RCP8.5 of Kopp et al. (2014) as high as 1.9 m by 2100. Meanwhile, in Greenland, there are indications that processes already underway have the potential to lead to an accelerating high-end melt risk. Important changes in surface albedo are occurring in response to ice melt and associated unmasking and concentration of impurities in snow and ice (Tedesco et al. 2016). At the base of the ice sheet, important changes in ice dynamics are occurring, through interactions with surface runoff and a warming ocean, which may make the Jakobshavn Isbræ, Kangerdlugssuaq Glacier, and the Northeast Greenland ice stream vulnerable to marine ice sheet instabilities (Khan et al., 2014).

The growing evidence of accelerated ice loss from Antarctica and Greenland only strengthens an argument for considering worst-case scenarios in coastal risk management. Miller et al. (2013) and Kopp et al. (2014) discuss several lines of arguments that support a plausible worst-case GMSL rise scenario in the range of 2.0 m to 2.7 m by 2100: (1) The Pfeffer et al. (2008) worst-case scenario assumes a 30-cm GMSL contribution from thermal expansion. However, Sriver et al. (2012) find a physically plausible upper bound from thermal expansion exceeding 50 cm (an additional ~20-cm increase). (2) The ~60 cm maximum contribution by 2100 from Antarctica in Pfeffer et al. (2008) could be exceeded by ~30 cm, assuming the 95th percentile for Antarctic melt rate (~22 mm/year) of the Bamber and Aspinall (2013) expert elicitation study is achieved by 2100 through a linear growth in melt rate. (3) The Pfeffer et al. (2008) study did not include the possibility of a net decrease in land-water storage due to groundwater withdrawal; Church et al. (2013) find a likely land-water storage contribution to 21st century GMSL rise of -1cm to +11 cm. Thus, to ensure consistency with the growing number of studies supporting upper GMSL bounds exceeding Pfeffer et al. (2008)'s estimate of 2.0 m by 2100 (Sriver et al., 2012; Bamber and Aspinall, 2013; Miller et al., 2013; Rohling et al., 2013; Jevrejeva et al., 2014; Grinsted et al., 2015; Jackson and Jevrejeva, 2016; Kopp et al., 2014) and the potential for continued acceleration of mass loss and associated additional rise contributions now being modeled for Antarctica (e.g., DeConto and Pollard, 2016), this report recommends a revised worst-case (Extreme) GMSL rise scenario of 2.5 m by 2100.

As for the lower-end scenario of 0.2 m by 2100 of Parris et al. (2012), this report now recommends this value be revised upward to 0.3 m by 2100, for several reasons. The primary reason is that the GMSL rise rate as measured by satellite altimeters has been tracking >3 mm/year for almost a quarter-century, mostly fluctuating with interannual variability associated with ENSO (Nerem et al., 2010; Boening et al., 2012; Fasullo et al., 2013; Cazenave et al., 2014). In addition, over the last 30 years (since the mid-1980s), tide-gauge-based reconstructions of GMSL (Church and White, 2011; Hay et al., 2015), which are in close agreement with the altimeter record since 1993, continue to report trends of ~3 mm/year. Continuation of this rate throughout the 21st century results in a GMSL rise of at least 0.3 m. The altimeter record and most recent 30-year record of tide-gauge-GMSL reconstructions are longer than the 19-year epoch used by NOAA to update their mean sea level tidal datum (performed to ensure accurate charting for safe navigation), and the altimeter record is nearing NOAA's 30-year requirement to compute a local RSL rate trend (Zervas, 2009). Lastly, even under the lowest of the RCPs (RCP2.6), which entails net-zero greenhouse gas emissions in the third quarter of this century and net anthropogenic removal of carbon dioxide from the atmosphere thereafter, multiple probabilistic studies (Kopp et al., 2014, 2016a; Mengel et al., 2016) indicate that GMSL is very likely (>90% probability) to still increase by 25–30 cm.

4.0 REGIONALIZATION OF THE GMSL RISE SCENARIOS

This section describes regional-scale climatic and nonclimatic factors that cause sea level to change regionally. Knowledge of these processes is applied to the global scenarios to develop integrated projections of regional sea level change.

4.1 Processes Affecting Regional RSL Change

As discussed earlier, GMSL rise is primarily driven by thermal expansion of the ocean as it warms and from increases in ocean mass from melting ice locked in mountain glaciers and polar ice sheets, with a secondary contribution from net changes in land-water storage. But a range of other factors also affect local-to-regional RSL (i.e., equation 1), whether by changing SSH, VLM, or both, as recently reviewed by Kopp et al. (2015):

- Changes in land-ice mass (e.g., melting glaciers and ice sheets) and in land-water storage not only change ocean mass and thus GMSL, but also 1) alter SSH with regionally distinct signatures from changes in the Earth's gravitational field and rotation, and 2) lead to regional VLM from flexure of the Earth's lithosphere. Collectively, these processes give rise to static-equilibrium fingerprints that characterize the spatial patterns of different mass transfers.
- Freshwater additions from land-ice melt or precipitation changes, as well as changes in the distribution of heat in the ocean and atmosphere, also alter regional SSH from altered oceanic and atmospheric processes involving the density, circulation, and distribution of water within the ocean.
- GIA, the ongoing response of the solid Earth to land-ice shrinkage at the end of the last ice age, drives post-glacial rebound under the core of the old ice sheets and subsidence on the margins leading to regional VLM, and secondarily also changes SSH regionally due to associated effects on the Earth's gravitational field and rotation, as well as on the overall volume of the ocean basin.
- Tectonics and sediment compaction, which occur from both natural causes and extraction of fluids like groundwater or hydrocarbons from sedimentary reservoirs, also drive VLM. These changes can be punctuated (not steady through time, e.g., earthquake-related or discontinued anthropogenic resource extraction) and more localized in nature.

In terms of future rise, the GMSL scenarios and gridded RSL responses are composed of 19-year average estimates reported on a decadal basis through 2100 (and subsequently for 2120, 2150 and 2200). In this context, interannual effects (e.g., ENSO) are negligible and multidecadal effects (e.g., PDO) are mostly attenuated or unresolved. Regional RSL projections or scenarios that account for static-equilibrium fingerprints, oceanographic processes, and VLM have been considered in several recent studies (Mitrovica et al., 2011; Yin, 2012; Perrette et al., 2013; Church et al., 2013a; Kopp et al., 2014, 2016a; Horton et al. 2015; Slangen et al., 2014; Grinsted et al., 2015; Hall et al., 2016). Results of the regionalization process are shown in section 5.

4.2 Regionalization Method

Projecting future RSL change requires accounting for a set of processes affecting SSH and VLM and their different spatial patterns in a fashion that is consistent with the magnitude of the projections of GMSL rise. Tasked to deliver local RSL rise scenarios, Hall et al. (2016) assessed all DoD installations worldwide within 20-km of a tidally influenced body of water to provide screening-level estimates of related vulnerabilities. They formulated site-specific RSL scenarios by Monte-Carlo

resampling of gridded climate-related data from Perrette et al. (2013) and Kopp et al. (2014) to weight their resultant samples per their specific set of GMSL rise targets for 2100. Hall et al. (2016) also applied VLM adjustments (based on datasets shown in Figure 5) to further localize the scenarios using rates from a global set of GPS measurements and derived from tide gauge platforms.

The basis for scenario development in this report is similar to the approach used by Hall et al. (2016), but distinct in that it uses regenerated datasets entirely based upon slight modifications of Kopp et al. (2014) to quantify RSL responses on a gridded basis (1-degree) for the U.S. coastline. (Projections are also provided at the precise locations of tide gauges.) To account for regional processes, the scenarios are based on probabilistic projections constructed for a set of contributory processes, which follow a framework and use data sources similar to those of Kopp et al. (2014). Key sources of information used in constructing each of these probability distributions are described in Table 2. Ice sheet mass changes were projected based on combining the IPCC expert assessment of likely ranges with information about the broader probability distribution from the expert elicitation of Bamber and Aspinall (2013). Glacier mass changes were based on a surface mass-balance model driven by an ensemble of Fifth Coupled Model Intercomparison Project (CMIP5) climate projections (Marzeion et al., 2012). Spatial patterns for the Greenland Ice Sheet, the West Antarctic Ice Sheet (WAIS), the East Antarctic Ice Sheet (EAIS), and 18 glacial regions' contributions to sea level rise were calculated following Mitrovica et al. (2011), assuming uniform melt across the source region (Figure 7). The assumption of uniform melt assumption may not be entirely realistic for the largest of the ice sources (Greenland, East Antarctica, and West Antarctica), but such an assumption would be more of a consequence to RSL near the ice source (Mitrovica et al., 2011) and generally not an issue for most of the U.S. Thermal expansion and ocean dynamics were based on a distribution constructed from the CMIP5 ensemble of global climate model projections (Taylor et al., 2012). The global-mean anthropogenic land-water storage contribution, which is a small contributor, was assumed to be spatially uniform and estimated based on the historical relationship between population size, retention of water in dams, and groundwater extraction, combined with United Nations (2014) population projections (Kopp et al., 2014).

To estimate the long-term contribution of nonclimatic processes such as GIA, tectonics, and sediment compaction to RSL change, we use results from a spatiotemporal statistical model of tide gauge data based upon methods described in Kopp et al. (2014). In this model, the spatiotemporal field of RSL change over 1900–2012 is represented as the sum of three signals: 1) a globally uniform sea level change, 2) a constant-rate average, long-term, regionally varying trend, and 3) temporally and spatially varying regional sea-level contributions. This model is separately fitted to tide gauge data in several different regions (of primary relevance to this analysis: the U.S. and Canadian Atlantic Coast, the Gulf of Mexico, the contiguous U.S. Pacific Coast, Alaska, and the Atlantic and Pacific Islands State and Territories). The spatial scales of variability of processes 2 and 3, and the temporal scale of variability of process 3, are learned in each region from the tide gauge data. The globally uniform signal is assumed to match the GMSL signal estimated by Church and White (2011); the discrepancy among different estimates of this signal likely contributes ~0.2 mm/year (2 cm/century) uncertainty to estimates of the long-term background RSL trend, which is considered small enough to neglect. The nonclimatic background RSL trend used for forward projections is the second process estimated by this model. This trend is assumed to continue at a constant rate. This assumption is accurate for GIA, but likely less so for unsteady processes such as those resulting from tectonic processes and/or anthropogenic disturbances (e.g., subsurface fluid withdrawal), which may increase or decrease over time. Both the regional degree of spatial variability in the background RSL trend and the density of nearby tide gauges affects the magnitude of the standard error during trend computation at the center of each 1-degree grid point.

A 1-degree spatial grid was chosen, since this resolution is typically sufficient for many decision-making needs and is a useful intermediate scale between the large-scale sources of RSL (estimated from Global Circulation Models [GCMs]) and the inherently (in some cases) local-scale VLM-related processes. It should be noted that scenario projections of RSL are also generated for specific tide gauge locations, so where there is location-specific tide gauge data, higher resolution background rates are obtainable. Gridded RSL results without a background RSL signal are provided to allow for the use of alternative sources of information about this background rate of change (see equation 2 in section 5.3). Users interested in substituting local VLM estimates instead (e.g., derived from a specific GPS dataset) are reminded that, although background rates primarily reflect VLM, they do include a related SSH contribution as well. Comparative analysis (see section 5.4) between gridded GPS-derived VLM and background nonclimatic RSL rates reveal broad agreement along U.S. coastlines.

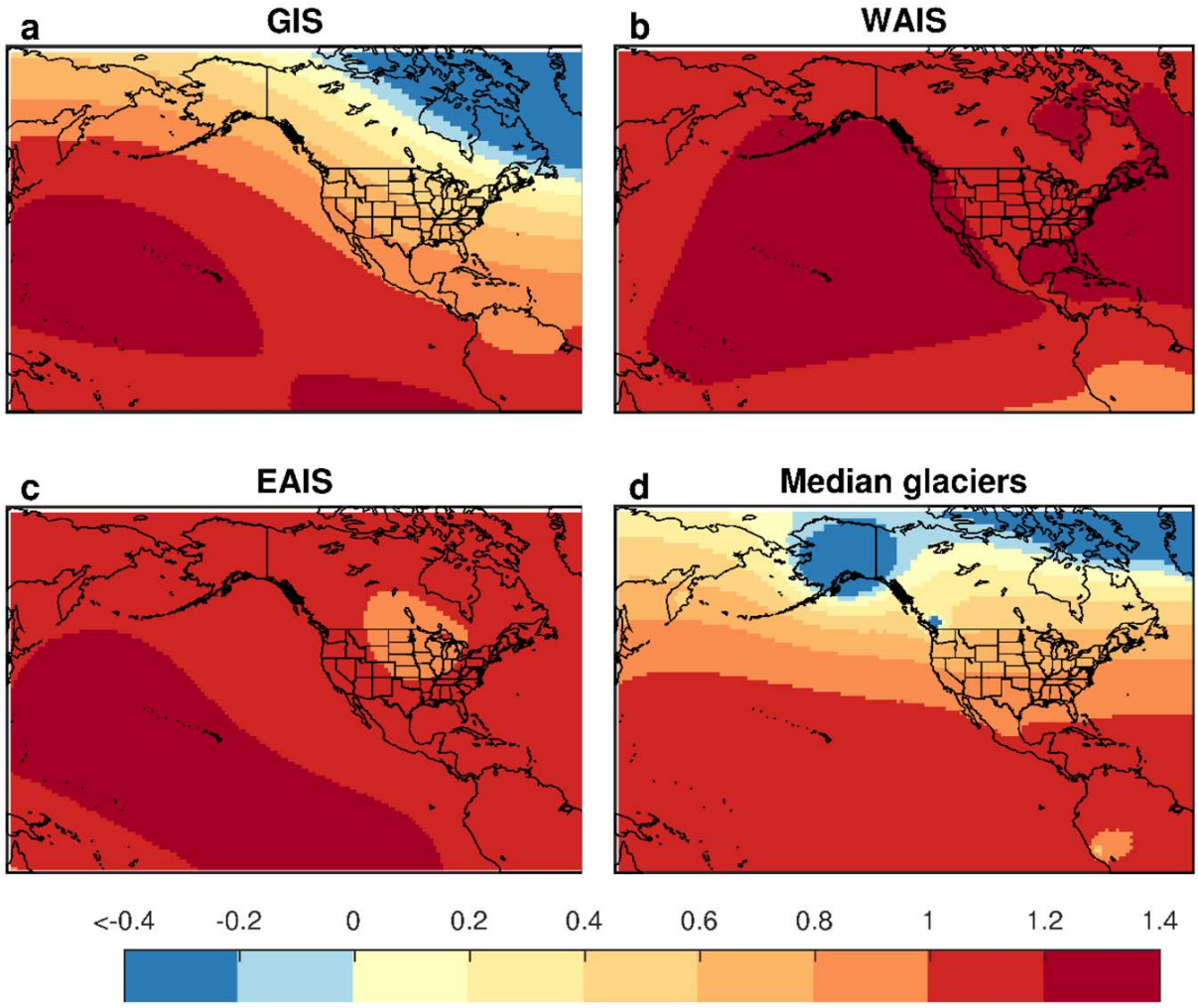

Figure 7. Ratio of RSL to GMSL change for mass loss from specific land-ice sources; these constitute the static-equilibrium fingerprints of the source. a) Greenland ice sheet (GIS), b) West Antarctic ice sheet (WAIS), c) East Antarctic ice sheet (EAIS) and d) the median of 18 mountain glaciers after Kopp et al. 2014, 2015. Values more than (less than) 1 indicate RSL rise higher (lower) than GMSL rise.

To tie the regional, probabilistic projections to the GMSL rise scenarios, 20,000 Monte Carlo-sampled time series of GMSL and regional RSL projections were generated for each of RCP2.6, RCP4.5 and RCP8.5 following the basic approach outlined by Kopp et al. (2014). Notable differences from Kopp et al. (2014) include 1) the use of the spatiotemporal statistical model described in that paper to estimate the background rate of change on a grid rather than exclusively at tide gauge sites, and 2) the use of the full spatial field of SSH projected by the CMIP5 GCMs to estimate the gridded responses. These projections were then pooled for the three RCPs considered and the results stratified into subsets as described in Table 3. Note that only the GMSL (and corresponding RSL) Monte Carlo estimates that fell within the prescribed range per scenario (e.g., 50 ± 2 cm for the 0.5-m scenario) were utilized, and thus the total number of samples shown in Table 3 do not equal the overall number of Monte Carlo samples. Finally, the median of the stratified subset of projections was taken to determine the time-evolution of GMSL for each scenario and the associated projections of RSL change.

To account for uncertainty in the relationship between GMSL and climate-related RSL, the central (i.e., median scenario value) and the 66th-percentile range corresponding to the 17th percentile (low scenario value) and 83rd percentile (high scenario value) of each stratified subset are also computed. To generate low, medium and high total RSL (climatic and nonclimatic contributions combined) sub-scenarios for each GMSL scenario in a way that allows easy substitution of alternative background RSL rate estimates, we combine the 17th percentile (low), 50th percentile (median) and 83rd percentile (high) of climatic RSL with, respectively, the 17th, 50th, and 83rd percentile of the background RSL rate contribution. The probability range (conditional upon the GMSL scenario) spanned by the total RSL sub-scenarios is therefore roughly 80%, with the precise range depending on the shape of the climatic RSL distribution. (If it were normally distributed, which it is not, it would be 84%.)

One additional modification of the Kopp et al. (2014) framework was required for the Low scenario. Within each RCP, the Kopp et al. (2014) framework incorporates a correlation between global mean thermal expansion and regional ocean dynamics derived from the CMIP5 archive. This correlation has the potential to create a significant discontinuity in ocean dynamics and thus in RSL projections across 2100 in the Low scenario. This is because RCP2.6 is dominantly responsible for the Low scenario, yet the number of CMIP5 simulations for RCP2.6 drops from 21 to six after 2100. This large drop leads to a discontinuity in the correlation between thermal expansion and ocean dynamics, and thus to a discontinuity in ocean dynamics, between 2100 and 2110. Since the contributions of thermal expansion and ocean dynamics are large relative to other terms in the Low scenario, this discontinuity appears particularly significant. To ameliorate this effect, we assume in the Low scenario that ocean dynamics are not correlated with global mean thermal expansion, except inasmuch as both terms depend upon emissions pathway.

Table 2. Key processes contributing to RSL and GMSL change, and sources of information.

Process	Affects SSH	Affects VLM	Sources of information used
Ice sheet mass changes	X	X	IPCC AR5 assessment of likely [>66% probability] ranges (Church et al., 2013a), with expert elicitation (Bamber and Aspinall, 2013) used to inform shapes of distribution tails; spatial patterns per Mitrovica et al. (2011)
Glacier mass changes	X	X	Glacier surface mass-balance model (Marzeion et al., 2012) driven by CMIP5 models; spatial patterns per Mitrovica et al. (2011)
Oceanographic processes (thermal expansion and atmosphere-ocean dynamics)	X		CMIP5 models (Taylor et al., 2012), with 5–95% range interpreted as likely range per IPCC convention
Land-water storage	X	X	Empirical relationships between population, dam storage, and groundwater withdrawal; uniform spatial pattern assumed
Glacial isostatic adjustment	X	X	Long-term background rate of RSL change inferred from spatiotemporal model of tide gauge observations
Tectonics and sediment compaction		X	Long-term background rate of RSL change inferred from spatiotemporal model of tide gauge observations

Table 3. Constraints used to stratify the projections and number of sample estimates per scenario. Note the definition of the Low scenario is the continuation of the current rate of GMSL rise (~3 mm/year) through 2100, whereas the others are just defined by 2100 values.

GMSL rise Scenario	Constraints	Number of samples
Low	2100 GMSL of 30 ± 2 cm; 2050 GMSL of 15 ± 2 cm; 2030 GMSL of 9 ± 1 cm	224
Intermediate-Low	2100 GMSL of 50 ± 2 cm	4407
Intermediate	2100 GMSL of 100 ± 2 cm	1040
Intermediate-High	2100 GMSL of 150 ± 5 cm	168
High	2100 GMSL of 200 ± 5 cm	23
Extreme	2100 GMSL of 250 ± 15 cm	21

As will be described in the next section, stratifying the probabilistic projections into six subsets in this way creates six scenarios (or families of scenarios) for GMSL and/or RSL at a given grid point (and set of tide gauge locations). It is important to emphasize that these six scenarios were not necessarily chosen to be relevant for any specific planning or decision-making process, nor to meet the needs of any specific decision-maker or other user, and the names (Low, High, etc.) are for convenience in usage. Section 6 provides discussion and guidelines for selecting the appropriate scenario from among these six—more broadly, from the full conditional probability distributions that these scenarios span— for a specific application and decision context. These particular scenarios do have meaning in a scientific context. The Low and Extreme scenarios represent the scientifically plausible lower and upper bounds on 21st century GMSL rise, respectively, as defined in this report; the remaining four scenarios (from Intermediate-Low to High), while simply placed at 0.5-m intervals in between, can be shown to correspond to different likelihood levels under RCP2.6, RCP4.5, and RCP8.5, as discussed in section 5.

5.0 RESULTS

There are a few important distinctions between the GMSL rise scenarios in this report and those of Parris et al. (2012) and Hall et al. (2016). Namely, the new scenarios: 1) are anchored in year 2000 (i.e., a 1991–2009 epoch), instead of 1992 (i.e., the National Tidal Datum Epoch of 1983–2001) so as to align with the framework of Kopp et al. (2014) and other sea level rise projections provided in the scientific literature, 2) provide decadal-scale estimates through 2100, 3) have a broader and higher range for GMSL rise by 2100 (0.3–2.5 m) as described above, 4) provide estimates through the year 2200, and 5) are downscaled to a 1-degree gridded basis to provide a systematic spatial framework to more broadly support regional/local decision making.

In terms of (1) above, we recognize that most of the U.S. is currently on a 1983–2001 datum epoch, and a RSL-change adjustment is needed for many applications. To obtain a 1991–2009 epoch (centered on year 2000) for a location, we suggest two methods. First, if a local tide gauge exists with RSL data over 1983–2009 exists, the simplest approach is to calculate the difference between the 1983–2001 average and the 1991–2009 average and then to apply this difference (NOAA, 2003). Second, if no adequate nearby tide gauge is available, an estimate of 8-years' worth of background RSL change (see section 5.4) can be combined with (a) an estimate of 8-years' worth of SSH change over 1992–2009, measured offshore by satellite altimetry, (b) a tide-gauge-based estimate of GMSL change between 1983–2001 and 1991–2009 (1.8 cm per Hay et al., 2015), or (c) an altimetry-based estimate of 8-years' worth of GMSL change at the rate characterizing 1993–2009 (3.0 cm per Nerem et al., 2010).

5.1 Global Mean Sea Level Rise Scenarios

As listed in Table 3, the six representative GMSL rise scenarios range from a low-end (Low) scenario of 0.3 m to a worst-case (Extreme) scenario of 2.5 m by 2100. The Intermediate-Low (0.5 m), Intermediate (1.0 m), Intermediate-High (1.5 m) and High (2.0 m) scenarios are the same as those put forward by Hall et al. (2016). In Figure 8, temporal evolution of the scenarios is illustrated through year 2100 relative to GMSL reconstructions from 1800 to 1900 based upon the meta-analysis of geological and tide gauge data of Kopp et al. (2016a), from 1900 to 2010 from the tide gauge analysis of Hay et al. (2015), and from 1992–2015 based upon satellite altimetry analysis updated from Nerem et al. (2010). The six GMSL rise scenarios are also shown (Table 4) relative to the probability of exceedance in 2100 as assessed by the RCP-based probabilistic projections of Kopp et al. (2014). Note that the GMSL rise scenarios assume that the rate of ice-sheet mass loss increases with a constant acceleration; however, this might not be the case (DeConto and Pollard, 2016), so it is, for example, possible to be on the Intermediate scenario early in the century but the High or Extreme scenario late in the century. Under the methodological assumptions of Kopp et al. (2014), in 2100 the Low scenario has a 94% to 100% chance of being exceeded under RCP2.6 and RCP8.5, respectively, whereas the Extreme scenario has a 0.05% to a 0.1% chance of being exceeded. However, as discussed in section 3, new evidence regarding the Antarctic ice sheet, if sustained, may significantly increase the probability of the Intermediate-High, High, and Extreme scenarios, particularly for RCP8.5 projections based upon Kopp et al. (2014). These ice-sheet modeling results have not yet been incorporated into a (conditional) probabilistic analysis of GMSL.

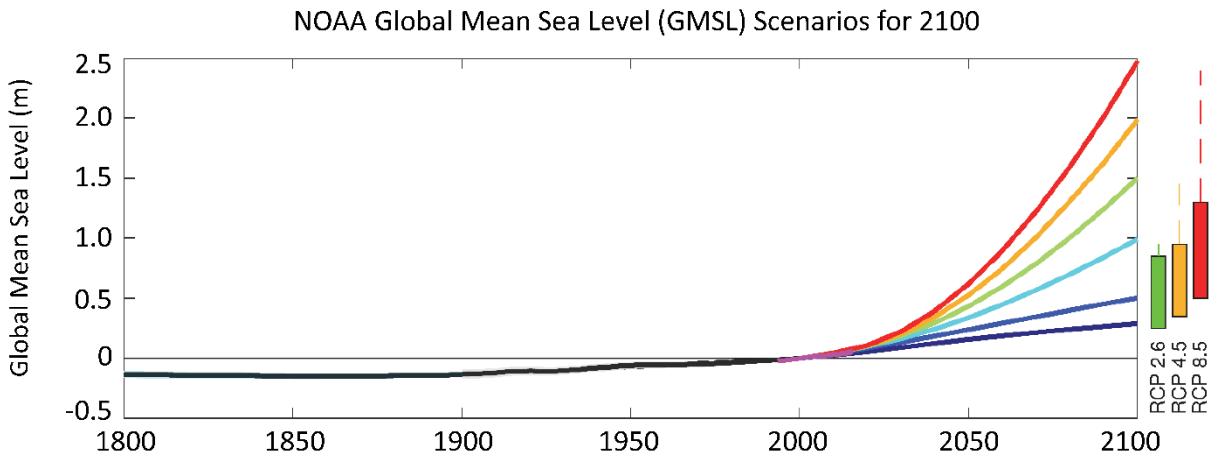

Figure 8. This study's six representative GMSL rise scenarios for 2100 (6 colored lines) relative to historical geological, tide gauge and satellite altimeter GMSL reconstructions from 1800–2015 (black and magenta lines; as in Figure 3a) and central 90% conditional probability ranges (colored boxes) of RCP-based GMSL projections of recent studies (Church et al., 2013a; Kopp et al., 2014; 2016a; Slangen et al., 2014; Grinsted et al., 2015; Mengel et al., 2016). These central 90% probability ranges are augmented (dashed lines) by the difference between the median Antarctic contribution of Kopp et al. (2014) probabilistic GMSL/RSL study and the median Antarctic projections of DeConto and Pollard (2016), which have not yet been incorporated into a probabilistic assessment of future GMSL. (A labeling error in the x-axis was corrected on January 30, 2017).

Table 4. Probability of exceeding GMSL (median value) scenarios in 2100 based upon Kopp et al. (2014).

GMSL rise Scenario	RCP2.6	RCP4.5	RCP8.5
Low (0.3 m)	94%	98%	100%
Intermediate-Low (0.5 m)	49%	73%	96%
Intermediate (1.0 m)	2%	3%	17%
Intermediate-High (1.5 m)	0.4%	0.5%	1.3%
High (2.0 m)	0.1%	0.1%	0.3%
Extreme (2.5 m)	0.05%	0.05%	0.1%

5.2 GMSL Rise Rates this Century and Rise Beyond 2100

Though the GMSL rise scenarios are primarily framed for overall changes occurring by 2100, it is important to recognize that GMSL rise will not stop at 2100; rather, it will continue to rise for centuries afterwards (Levermann et al., 2013; Kopp et al., 2014). By 2200, the 0.3–2.5 m range spanned by the six GMSL rise scenarios increases to 0.4–9.7 m, as shown in Table 5. It can be seen (Figure 8) that deceleration of GMSL occurs under the Low scenario with only slight increases through 2200. Continued acceleration is modest under the Intermediate-Low scenario and pronounced under all other scenarios (Table 6). The amount of GMSL rise by 2200 does not necessarily represent the maximum physically possible contributions from ice-sheet, ice-cliff or ice-shelf feedback processes, which, as discussed in section 3, may significantly increase contributions to overall GMSL rise amounts (DeConto and Pollard, 2016).

Table 5. GMSL rise scenario heights in meters for 19-year averages centered on decade through 2200 (showing only a subset after 2100) initiating in year 2000. Only median values are shown.

GMSL Scenario (meters)	2010	2020	2030	2040	2050	2060	2070	2080	2090	2100	2120	2150	2200
Low	0.03	0.06	0.09	0.13	0.16	0.19	0.22	0.25	0.28	0.30	0.34	0.37	0.39
Intermediate-Low	0.04	0.08	0.13	0.18	0.24	0.29	0.35	0.4	0.45	0.50	0.60	0.73	0.95
Intermediate	0.04	0.10	0.16	0.25	0.34	0.45	0.57	0.71	0.85	1.0	1.3	1.8	2.8
Intermediate-High	0.05	0.10	0.19	0.30	0.44	0.60	0.79	1.0	1.2	1.5	2.0	3.1	5.1
High	0.05	0.11	0.21	0.36	0.54	0.77	1.0	1.3	1.7	2.0	2.8	4.3	7.5
Extreme	0.04	0.11	0.24	0.41	0.63	0.90	1.2	1.6	2.0	2.5	3.6	5.5	9.7

The rates of GMSL associated with the time-dependent GMSL rise heights are shown in Table 6. Rates range from a near-constant 3 mm/year of the Low scenario (by definition) this century to 5 mm to 44 mm/year later (2081–2099 average) in the century, with differing amounts of acceleration. As previously noted, global mean thermal expansion, ocean dynamics, and glacier melt in the Kopp et al. (2014) framework are derived from the CMIP5 archive (directly for thermal expansion and ocean dynamics, as an input to a glacier mass-balance model for glacier melt). The reduction in CMIP5 model simulations after 2100 leads to small discontinuities in GMSL and RSL between 2100 and 2110. We therefore advise caution when using projections for 2110 and advise against calculating rates over periods spanning 2100. Accordingly, for the 22nd century, Table 5 focuses on projections for 2120, 2150, and 2200, and the rates in Table 6 are calculated only for the 21st century.

As for the actual GMSL scenario heights, it is possible to be on a rate associated with an Intermediate-Low or Intermediate scenario earlier in the century, but since the rate of ice-sheet mass loss may not necessarily change linearly (e.g., DeConto and Pollard, 2016), GMSL rise rates could transition to those associated with higher GMSL rise scenarios later in the century and could exceed all rates shown. For context, the geological record reveals that during the last deglaciation (~20,000–9000 years before the Common Era), GMSL rise rates exceeded about 10 mm/year, with rates above 40 mm/year during meltwater pulses (Deschamps et al., 2012; Miller et al., 2013).

Table 6. Rise rates (in millimeters per year for 19-year averages centered on decade) associated with the median GMSL scenario heights this century (as shown in Table 5).

GMSL Scenario Rates (mm/year)	2010	2020	2030	2040	2050	2060	2070	2080	2090
Low	3	3	3	3	3	3	3	3	3
Intermediate-Low	4	5	5	5	5	5	5	5	5
Intermediate	5	6	7	9	10	12	13	14	15
Intermediate-High	5	7	10	13	15	18	20	22	24
High	6	8	13	16	20	24	28	31	35
Extreme	6	10	15	20	25	30	35	40	44

5.3 Regional Climate-related RSL Changes

The amount of RSL change that occurs regionally under each GMSL rise scenario reflects contributions from both 1) climate-related processes affecting regional SSH and VLM and 2) nonclimatic background RSL changes, primarily from VLM but also including any related SSH changes. In other words, for a given scenario,

$$2)\ \Delta RSL\ (x,t) = \ Climatic\ \Delta RSL\ (x,t)\ +\ Background\ RSL\ rate\ (x)\ (t - t_0)$$

where ΔRSL, the total RSL change relative to RSL at time t_0 in the sea level scenario, is defined for spatial locations *x* and times *t*, and the nonclimatic, background change is assumed to be linear in time.

The climatic and nonclimatic responses are quantified separately to allow supplemental VLM estimates (e.g., local GPS measurements) to be substituted for the background RSL rate estimates instead. However, one caution as stated earlier is that using localized GPS-VLM rate estimates in place of the tide gauge-estimated background rates may lead to the neglect of any SSH effects within the background RSL rate. These effects can be significant; for instance, in some GIA models (e.g., Peltier, 2004), SSH fall offsets about one-third of the RSL rise caused by land subsidence in New York City.

Figure 9 shows how the median climate-related RSL projections at 1-degree resolution for each scenario in 2100 differ from the median GMSL rise for that scenario. This difference can be either positive or negative; i.e., the climatic contribution to RSL change can be either greater or less than the GMSL rise, with differences between the climate-related RSL change and GMSL rise arising due to both ocean dynamics (e.g., along East Coast) and the static-equilibrium fingerprint effects of land-ice mass changes. In addition to the median value, low and high RSL values for each GMSL rise scenario are shown in appendices B and C, for climate-related (not including background) and total RSL, respectively. The climate-related RSL projection patterns in Figure 9 are summarized with those of the nonclimatic background RSL rates later in section 5.5.

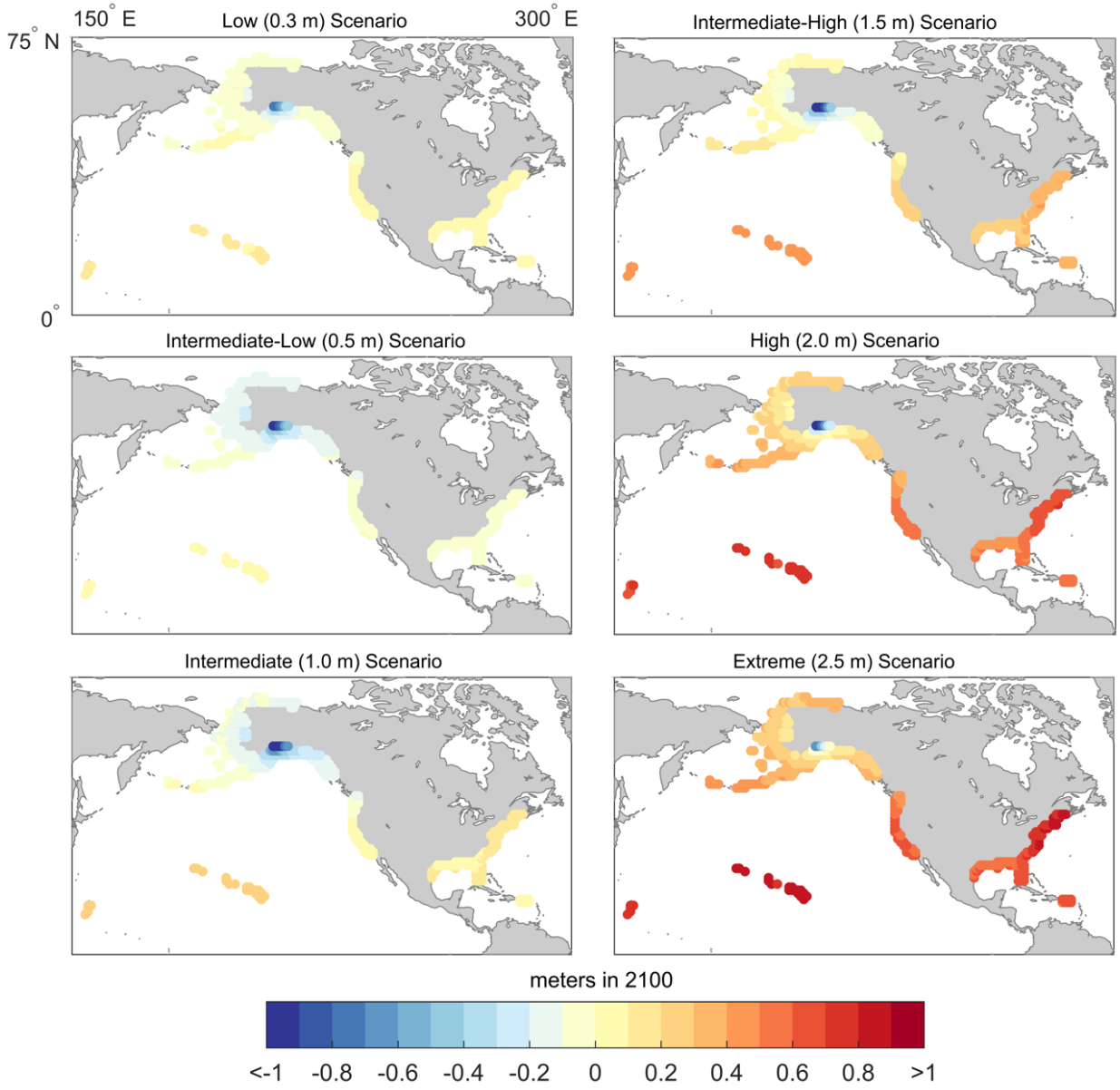

Figure 9. Climate-related RSL change at 1-degree resolution for 2100 (in meters) relative to the corresponding (median-value) GMSL rise amount for that scenario. To determine the total climate-related RSL change, add the GMSL scenario amount to the value shown.

Figure 10 shows several key components that contribute to the median RSL projections using the Intermediate (1-m GMSL) scenario as an example. Note that this figure shows the total contribution of a process to RSL change, not just the difference from GMSL change as in Figure 9. Accounting for the amplification of its contribution by static-equilibrium processes (Figure 7), the Antarctic Ice Sheet (AIS) contributes 0.1–0.2 m to RSL rise across the U.S. The Greenland Ice Sheet (GIS) contributes 0.1–0.2 m as well across most of the U.S., with higher (0.2–0.3 m) amounts within the Pacific due to far-field static-equilibrium effects and lower amounts (0–0.1 m) along the Northeast Atlantic and Northern Alaska due to intermediate-field effects. (Both AIS and GIS progressively contribute to higher RSL rise along most U.S. shorelines, with similar patterns under the Intermediate-High, High and Extreme scenarios). RSL contributions from glacier and ice caps (GIC) melt are about 0.2 m from melt around the U.S., but are substantially lower (sizable RSL fall in some places) due to near-field and intermediate-field static-equilibrium effects along the Alaskan coast and in the Pacific Northwest.

Lastly, oceanographic (OC) processes, including both global mean thermal expansion and regional atmosphere/ocean dynamics, contribute about 0.4–0.5 m to RSL rise around the U.S. and higher along the Northeast Atlantic Coast (0.7–0.8 m) related to changes in the Gulf Stream System.

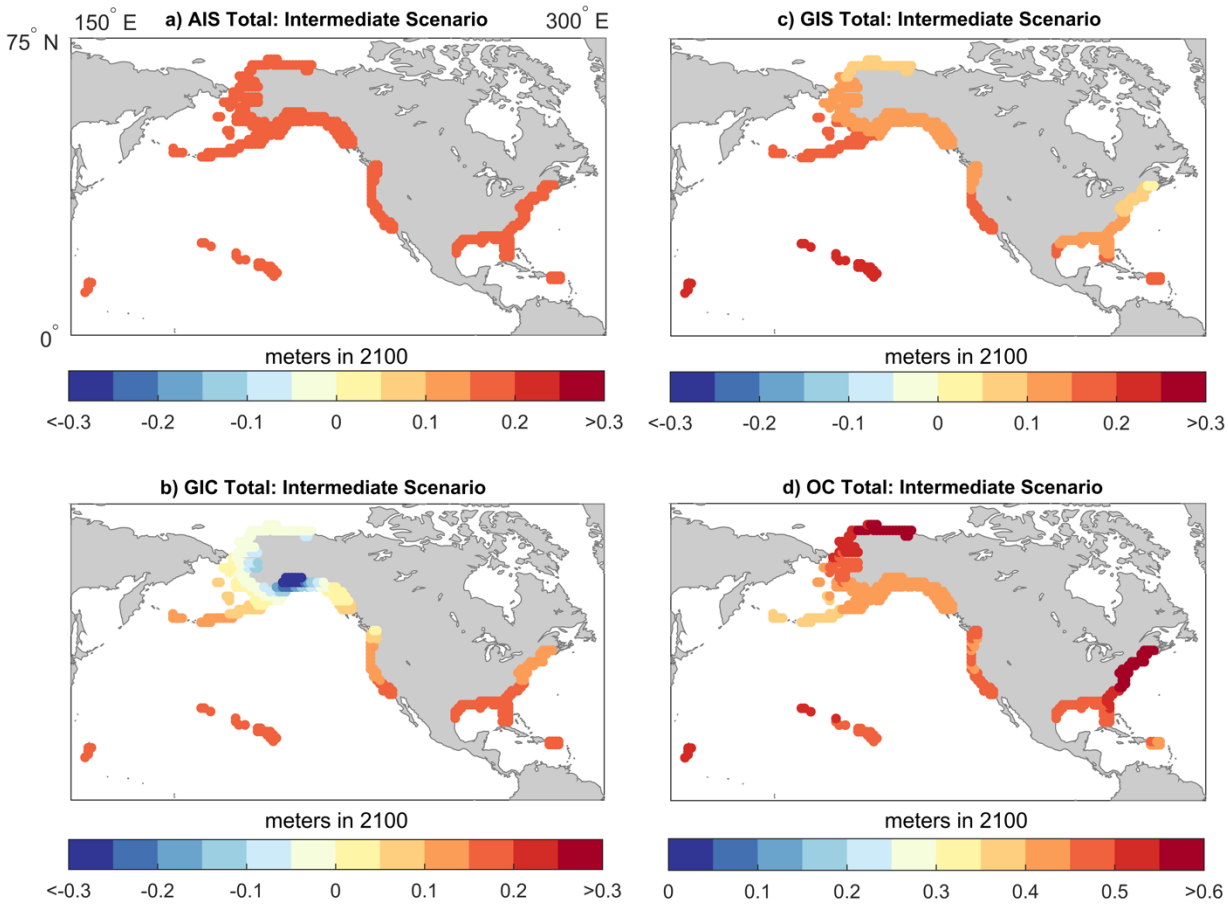

Figure 10. Component contributions (in meters) to the median RSL Intermediate (1.0 m GMSL rise) scenario values in 2100 from a) the AIS, b) GIC, c) GIS and d) oceanographic processes (global mean thermal expansion and regional atmosphere/ocean dynamics; note that a different scale is used).

Figure 11 compares the median climate-related RSL values shown in Figure 9 for the Intermediate (1-m GMSL rise) scenario for the year 2100 to those of Hall et al. (2016). For this comparison, the Hall et al. (2016) 1-m sea level scenario has been gridded (Figure 11a). Similar patterns emerge, such as higher values along the Hawaiian coastline due to far-field effects from Antarctic ice-mass loss; lower values (negative) occur along the Alaskan and Northwest U.S. coasts from near-field effects of ice-mass loss of Alaskan mountain glacier and Greenland melt. Because of differences between the methods used in this report as compared to those in Hall et al. (2016), some variations are expected. Notable differences between this study's results (Figure 11b) include higher values (10–20 cm) along the U.S. East Coast and generally higher values along the Southern Alaskan Coast (50 cm or more) than the Hall et al. (2016) values. This may be due to Hall et al. (2016)'s usage of a single fingerprint for all glaciers combined, or to somewhat different Alaska fingerprint values in the Alaska regions of Perrette et al. (2013) used in the Hall et al. (2016) study. Perrette et al. (2013) relied on the present-day distribution of mass loss using the model of Bamber and Riva (2010) to develop fingerprints, which were assumed to remain the same in the future. Also, Hall et al. (2016) used only a single Antarctic fingerprint, which did not differentiate contributions from the WAIS (Figure 7). This may account for their lower values along North America, since the WAIS fingerprint has a higher relative effect than

the EAIS along both coasts. Another source of difference could be related to a higher overall contribution from Greenland in the Hall et al. (2016) study, which, due to near- and intermediate-field static equilibrium effects (Figure 8a), would cause a reduction of climate-related RSL along the U.S. East Coast as seen in Figure 11a. On average, this study's gridded values for the Intermediate scenario are 8 cm higher along the U.S. coastline, though with similar RSL spatial patterns in general agreement (linear regression of RSL within grids for the Intermediate (1-m GMSL rise) in Figures 9 and 11a: R^2=0.65).

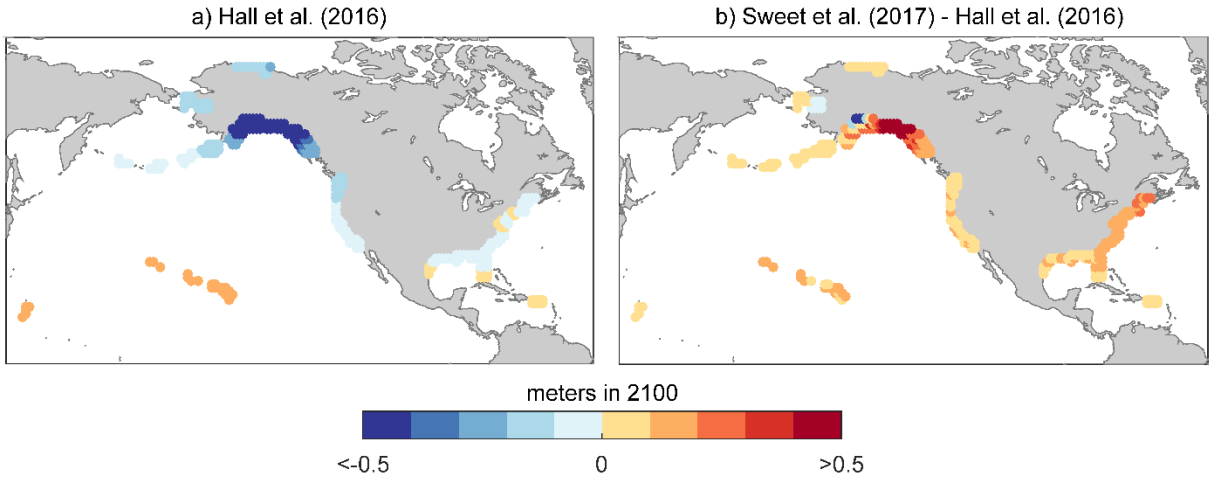

Figure 11. a) Median climate-related RSL amounts under the Intermediate (1-m GMSL rise) scenario in year 2100 of Hall et al. (2016) (with all grid values shown with GMSL amount [1.0 m] removed) and b) difference between RSL in this study's (Sweet et al., 2017) Intermediate scenario as shown in Figure 9 and Hall et al. (2016) results shown in a).

5.4 Nonclimatic Background RSL and GPS VLM Trends

The other factor needed to regionalize the GMSL rise scenarios is background RSL change caused by nonclimatic processes. These background changes are primarily driven by VLM, but also include SSH changes associated with GIA. The gridded background RSL trends, which are assumed to measure linear trends and to be independent of scenario, are shown in Figure 12a. The assumption of background RSL rate persistence this century is valid for risk-framing purposes (Hall et al., 2016) but could become invalid if, for example, most of the underlying signal stems from anthropogenic-induced VLM, and the driving disturbance ceases at some point in the future. The background RSL rates reveal similar patterns as the GPS-derived VLM estimates, which are shown in Figure 12b as a 1-degree gridded version of Figure 5 for GPS sites within 50 km of the U.S. coastline. Note that the direction of the GPS VLM rates have been switched in Figure 12b (and Figure 12e, f) for comparison purposes (i.e., negative VLM trends or downward motion of the land are shown as a positive contribution to RSL change). Common patterns between the tide gauge background RSL and GPS-VLM trend estimates include slight RSL fall (0 to 1 mm per year RSL fall/land uplift) along the U.S. West Coast. RSL rise/land subsidence rates of about 1–2 mm/year are found broadly along the U.S. East Coast, though this is higher (2–4 mm/year or more) along the Mid-Atlantic coast from Virginia to New Jersey due to a combination of both anthropogenic processes, such as extraction of groundwater, and GIA associated with the disappearance of the North American (Laurentide) Ice Sheet. Within the central and western Gulf of Mexico, RSL rise/land subsidence rates of about 3–5 mm/year or more reflect sediment compaction of the Mississippi River Delta and withdrawal of subsurface groundwater and fossil fuels. RSL fall/land uplift rates of 5 mm/year or more are found in Southern Alaska due in part to GIA associated with the post-Little Ice Age retreat of mountain glaciers.

Figures 12c and 12d show the standard deviations of the background RSL and VLM rate trends, which are approximately 1–2 mm/year within the continental U.S. and generally higher along the Alaskan Coast as assessed by tide gauges. Trend standard deviations from the tide gauges (Figure 12c) are generally less along the contiguous U.S. as compared to those derived from GPS (Figure 12d), likely due to much shorter GPS record lengths as compared to the tide gauges. As detailed in section 4.2, the spatial scale of variability of the background RSL trend is learned from the data, which is why the errors are much larger farther away from tide gauges in Alaska (where gauges are sparse and the dominant spatial scale of variability short) than on the U.S. East Coast (where gauges are numerous and the dominant spatial scale of variability long). Similarly, VLM rates and their uncertainties assessed by GPS will vary, often substantially over relatively short distances. A reason why the standard deviations of the gridded VLM trends are relatively low in Alaska (Figures 12d) is due to the computation process. Unlike the background RSL trend, which is estimated for the specific center of the grid, the VLM rates and their standard deviations are derived by simply pooling available measurements, averaging their rates, and statistically reconciling the trend variances.

Figure 12e shows the differences in rates between the background RSL and GPS VLM trends. Larger discrepancies occur in regions where rates are high and likely influenced by human activities that have varied through time, such as pumping of groundwater/fossil fuels (e.g., Western Gulf of Mexico); discrepancies are also high where large spatial-differential VLM rates exist due to processes such as volcanism, tectonics or recent glacier retreat (e.g., Southern Alaska). However, the trend rates derived from tide gauge (background RSL) and GPS (VLM) are generally in close agreement (±1 mm/year) along much of the U.S., which is further exemplified by the high goodness of fit measure in Figure 12f (black dots: $R^2 = 0.78$). Also shown in Figure 12f is a similar comparison among the background RSL rates as in Figure 12a, but derived and compared to VLM estimated for more than 100 specific tide gauge locations used by Hall et al. (2016) and based upon Zervas et al. (2013). In this instance, the two data sets (shown as red dots) are quite close ($R^2 = 0.92$), with discrepancies partly because Zervas et al. (2013) use a constant 20th century GMSL rise rate instead of a time-varying rate corresponding to the specific time periods covered by the regional groups of tide gauges used in their assessment.

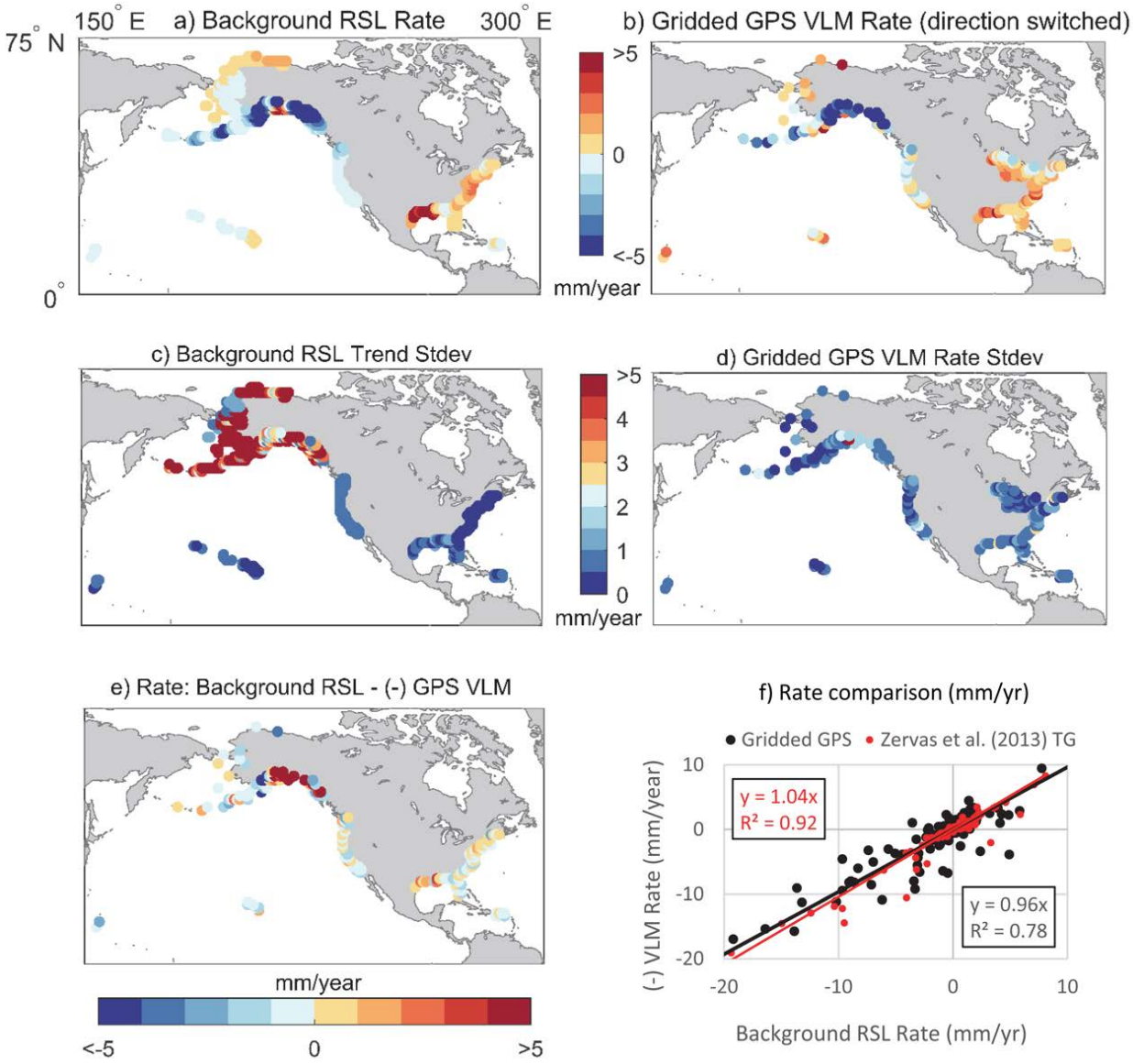

Figure 12. Gridded a) background RSL rates and b) GPS VLM rates (with directionality switched as to directly compare to RSL rate) with trend standard deviations shown in c) and d). In e) is the difference between the two rates shown in a) and b). In f) is a scatterplot and linear regression of the two sets of gridded rates shown in a) and b) as black dots and the red dots show background RSL rates as in a) but derived and compared to VLM estimated for more than 100 specific tide gauge (TG) locations used by Hall et al. (2016) and based upon Zervas et al. (2013).

5.5 Scenario Projections of Relative Sea Level (RSL)

Figure 13 shows the total median RSL projections relative to the median GMSL values for each scenario for 2100 (Figure 8). High and low RSL values for each GMSL scenario are provided for each scenario in appendix C. The patterns reflect those inherent to Figures 9 and 12a as summarized in section 5.3. For instance, under the Intermediate-High (1.5-m GMSL rise) scenario, RSL along the U.S. East Coast is about 0.4–0.7 m higher than GMSL rise, 0.2–1.0 m higher along the Gulf Coast, 0.2–0.3 m higher along the West Coast, 0.3–0.5 m higher within Hawaii and the Pacific Islands and both slightly higher and much lower (-1.0 m to +0.2 m) along the Alaskan Coast.

Some notable patterns projected to occur this century (Figure 13) and their physical interpretations (based on Yin, 2012; Perrette et al., 2013; Church et al., 2013a; Kopp et al., 2014, 2016a; Slangen et al., 2014; Grinsted et al., 2015) are listed below.

- Future RSL rise is amplified along the Northeast U.S. coast due to the effects of GIA, the far-field static equilibrium effects of Antarctic melt (Figure 7), and reduced transport of the larger Gulf Stream System (Atlantic Meridional Overturning Circulation [AMOC]). Future RSL rise is partially reduced by intermediate-field static-equilibrium effects associated with relative proximity to Greenland and many northern glaciers.
- RSL rise is amplified along the western region of the Gulf of Mexico and much of the Northeast Atlantic coast by withdrawal of groundwater (along the Atlantic Coast) and of both fossil fuels and groundwater (along the Gulf Coast). Continuation of these practices would amplify future RSL rise. Far-field static equilibrium effects of Antarctic melt (Figure 7) are also amplified in these two regions (as in the first bullet describing the Northeast U.S.).
- Future RSL is amplified along the Pacific Coast of the continental U.S. due to far-field static-equilibrium effects of Antarctic ice sheet melt.
- Future RSL is reduced along the Alaska and the U.S. Pacific Northwest coasts due to proximity to the Alaskan glaciers from both ongoing GIA to past glacier shrinkage and to the static-equilibrium effects of projected future losses.
- Future RSL rise is amplified in Hawaii and other Pacific islands by static-equilibrium effects, because they are in the far field of all sources of melting land ice.

It should be noted that the probabilistic construction of the High and Extreme scenarios draw more heavily on Antarctic contributions than might be the case in a world with 2.0 m or 2.5 m of GMSL rise by 2100, respectively. This is because: 1) There is no assumed correlation between Greenland and Antarctic melt other than that associated with the RCP forcing, 2) the High and Extreme scenarios require a large Antarctic contribution, and 3) under an assumption of noncorrelation, it is unlikely that both the Greenland and Antarctic contributions will be extreme. Because Antarctic contributions to RSL rise are amplified along all U.S. coastlines, while Greenland contributions are dampened across much of the U.S., RSL is projected to be higher than if driven by a more extreme Greenland contribution and a somewhat less extreme Antarctic contribution.

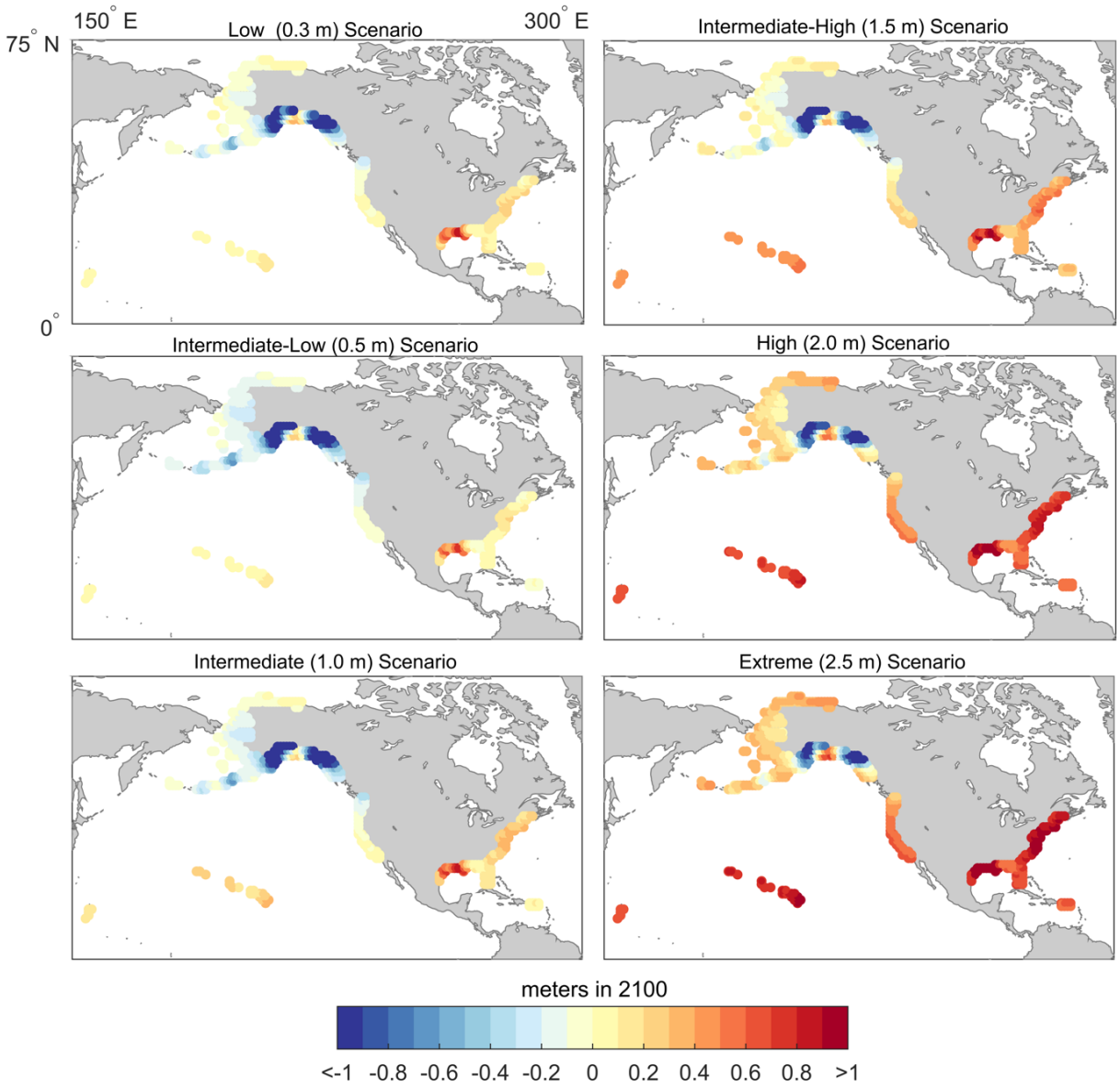

Figure 13. Total RSL change at 1-degree resolution for 2100 (in meters) relative to the corresponding (median-value) GMSL rise amount for that scenario. To determine the total RSL change, add the GMSL scenario amount to the value shown.

6.0 USAGE OF SCENARIOS WITHIN A RISK-BASED CONTEXT

Significant uncertainties exist about the exact trajectory (and impacts) of future climate change, limiting the value of prediction-based frameworks for long-term, climate-related decision-making (e.g., see Hallegatte et al. 2012, Weaver et al., 2013). In other words, decision-makers must expect to be surprised (NRC, 2009). Planning approaches using sea level scenarios (e.g., Parris et al., 2012 and Hall et al., 2016) can help manage uncertainty for continuity of mission and functionality of critical system(s). For example, long-term coastal planning at a local or regional/state level (e.g., major infrastructure upgrades) requires information about possible RSL rise that might affect the project in response to all factors associated with the warming of the oceans and cryosphere. Parris et al. (2012) did not explicitly provide such information, and although the Hall et al. (2016) study did, their site-specific results are not publicly available.

This report provides GMSL rise scenarios and associated 1-degree resolution RSL (amounts and rates) covering what is plausibly a full range of possible futures given current scientific understanding and different assumptions about future greenhouse gas emissions. However, further information is needed for their application, such as how best to identify and select the small number of most relevant scenarios for a specific management application from the full conditional probability distributions. Providing such guidelines in a tailored way across the diversity of coastal planning contexts is beyond the scope of this report. However, drawing upon Hall et al. (2016), Hinkel et al. (2015), Kopp et al. (2016b), King et al. (2015) and others, it is possible to put forth some general guidelines and provide a couple of different contextual examples.

6.1 General Guidelines for Scenario Selection

Coastal planners making critical decisions should weigh several factors, such as the type of decision to be made, expected future performance, planning horizon, and overall risk tolerance, including the criticality of the asset and/or the size and vulnerability of the exposed population (Hall et al., 2016). The process of selecting a sea level scenario for a specific setting is not a straightforward task for planners and engineers, and there are only a few case studies regarding its application in the literature (e.g., Hall et al., 2016; Ranger et al., 2013). Choosing meaningful sea level scenarios for risk management purposes begins with an understanding of the specific system, problem, goals, and preferences. These may include:

- What is the decision type? What is the operational timeframe over which the decision needs to function in an effective manner (planning horizon)? How flexible is the decision should new information become available?
- Who and what will be affected if sea level increases, and in what way? What is “at risk”?
- What outcomes are desired to avoid, in the near and long term with respect to these valued things? What is the tolerance for risk?
- Are there thresholds or tipping points in human or natural systems of concern beyond which damages would increase dramatically?
- What are the specific details of the coastal system: e.g., elevation, characteristics of the coastline, the locations of things of value (houses, infrastructure, sensitive ecosystems)?

Key to the decision process is determining the extent to which a given amount of RSL rise may cause impacts to either newly built or existing infrastructure. This will differ by geographic location due to differences in topography, land cover, physical forcing (i.e., affecting the width of the typical high water ‘distribution’ in Figure 1), and existing storm-flood defenses. Thus, it is important to recognize

the nature of the surrounding physical forcing regime and how the type of anticipated impact (e.g., magnitude, frequency or duration of high water event) might vary in the future under the range of sea level scenarios. A relatively small amount of RSL rise will substantially increase the frequency and spatial extent of flooding more in some locations than others. For instance, tidal flooding has and will continue to become more frequent and severe with a given amount of RSL rise along regions with flat, low-lying coastal zones that typically do not experience regular, severe storm surges (e.g., the Southeast Atlantic Coast) more so than along regions with steeper topography that experience often-severe extratropical storms (e.g., New England Coast) (Sweet and Park, 2014). Often, if a location is prone to impacts from severe storms, some flood defenses may likely be in place, such as for storm surges along a beachfront (e.g., seawalls, elevated houses along the beachfront). But back bay and inland regions of harbor cities with infrastructure (e.g., transportation, waste and stormwater systems) at ground level will continue to be exposed to impacts of more-probable and increasingly-extreme tidal flooding due to RSL rise.

Early stages of planning need to establish the conceptual linkage between sea level rise, the system(s) of interest, and the threat to those systems. Once a conceptual linkage is established, the next step is to "stress test" the system and the plans against different futures to assess potential risks. Scenarios, to be most useful, should delineate between policies or plans that succeed and those that fail (Lempert, 2013). For decisions involving long planning horizons and with a limited adaptive management capacity, the high degree of uncertainty in late-21st century GMSL rise looms large. Failure to adequately account for low-probability, high-consequence outcomes significantly increases future risks and exposure (Oppenheimer and Alley, 2016). For many decisions, it is essential to assess worst-case scenarios, not only those assessed as the scientifically 'likely' to happen. For example, drawing on the references cited above, the following is suggested as a potential initial scenario selection strategy for decisions and planning processes for which *long-term* risk management is paramount:

- Define a scientifically plausible upper-bound (which might be thought of as a worst-case or extreme scenario) as the amount of sea level rise that, while low probability, cannot be ruled out over the time horizon being considered. Use this upper-bound scenario as a guide for overall system risk and long-term adaptation strategies.
- Define a central estimate or mid-range scenario (given assumptions about greenhouse gas emissions and other major drivers). Use this scenario as baseline for shorter-term planning, such as setting initial adaptation plans for the next two decades. This scenario and the upper-bound scenario can together be thought of as providing a general planning envelope.

This approach is consistent with that recommended in Kopp et al. (2016b) and used by the Thames Estuary 2100 project (Ranger et al., 2013; Hinkel et al., 2015). Continuous monitoring of current sea level behaviors (trends and variability), along with improved scientific understanding of relevant climate-system processes and feedbacks, can then help identify the evolution of the system over time with respect to these mid-range and worst-case scenarios. Systematic assessments can determine current sea level rise (and risk) trajectories and when to implement more aggressive response options against the high-end scenario if adaptive management strategies are an option (USACE, 2013; Hall et al., 2016).

Several other logistical aspects should be considered, such as relevant elevation-frequency thresholds, probability of water level events (recurrent-to-rare in frequency), availability of spatial/mapping and tidal-geodetic datum information, rates of change, and other factors. The following sections provide

more detailed scenario applications that consider these additional factors, focused on increasing frequency of recurrent tidal flooding at a national scale and the increasing magnitude of a major flood event along the South Florida coast.

6.2 Scenario Projections of RSL and Tidal Flood Frequencies: A National Perspective

Impacts of RSL have been and will continue to be experienced as increasingly deep and frequent tidal flooding (e.g., Ezer and Atkinson, 2014; Sweet et al., 2014; Sweet and Park, 2014; Sweet et al., 2016). Tidal flooding is an impact event not generally attributed to a particular storm event, but rather from the continued effects of RSL rise, which elevate the reach of normal tides and water-level setup from prevailing winds. Eventually, the cumulative toll from recurrent tidal flooding above a local-specific physical threshold (i.e., duration, magnitude, or frequency) will eventually degrade sector-specific functionalities and/or exceed economic or public-tolerance thresholds. In the following example, we highlight how the frequency of tidal-flood frequencies may change in response to RSL rise (or fall) under the sea level scenarios. Our focus is on events that have been sufficiently sampled in time as to provide a robust understanding of their probability of occurrence. A similar assumption is commonly used when providing maps of future high tide levels associated with rising sea levels (e.g., NOAA Sea Level Rise Viewer: https://coast.noaa.gov/slr).

Recognizing a location's current RSL trajectory relative to its set of scenarios and past degree of interannual variability can assist in decision-making processes over the next several decades. Figure 14 shows observed annual mean RSL for four U.S. cities relative to future RSL under the six scenarios. In most circumstances, the range of interannual RSL change/variability since 2000 has been bounded (to date) by the trajectory of the Intermediate-High (1.5-m) scenario. As noted previously, it is important to recognize that being close to one scenario early in the century does not imply that real-world behavior will follow that scenario throughout the century; for example, rapid ice sheet collapse in Antarctica could conceivably bring the world from the Intermediate scenario early in the century to the Extreme scenario by the end of the century.

In places like San Francisco (and along the West Coast), interannual RSL variability over the last several decades has been and may continue to be large compared to the RSL trend itself (see tidesandcurrents.noaa.gov/sltrends). This can be counterintuitive especially for local decision-makers, since it suggests that historical trends in RSL may be a poor predictor of future sea level rise. Because there is not expected to be much difference in RSL under the scenarios over the next couple decades (Church et al., 2013a; Kopp et al., 2014), where yearly RSL variability effectively spans a large section of the range of (19-year average) scenarios, near-term decision-making (e.g., annual-to-decadal) may be effectively scenario-independent. In such circumstances, time-dependent event probabilities of both minor tidal flooding and more severe events respond primarily to RSL variability and/or climatic phases affecting regions such as by ENSO, the Atlantic Multidecadal Oscillation (AMO), the North Atlantic Oscillation (NAO), etc. (Menendez and Woodworth, 2010; Park et al., 2010; Sweet and Park, 2014; Marcos et al. 2015; Woodworth and Menendez, 2015; Wahl and Chambers, 2016; Sweet et al., 2016; Hall et al., 2016).

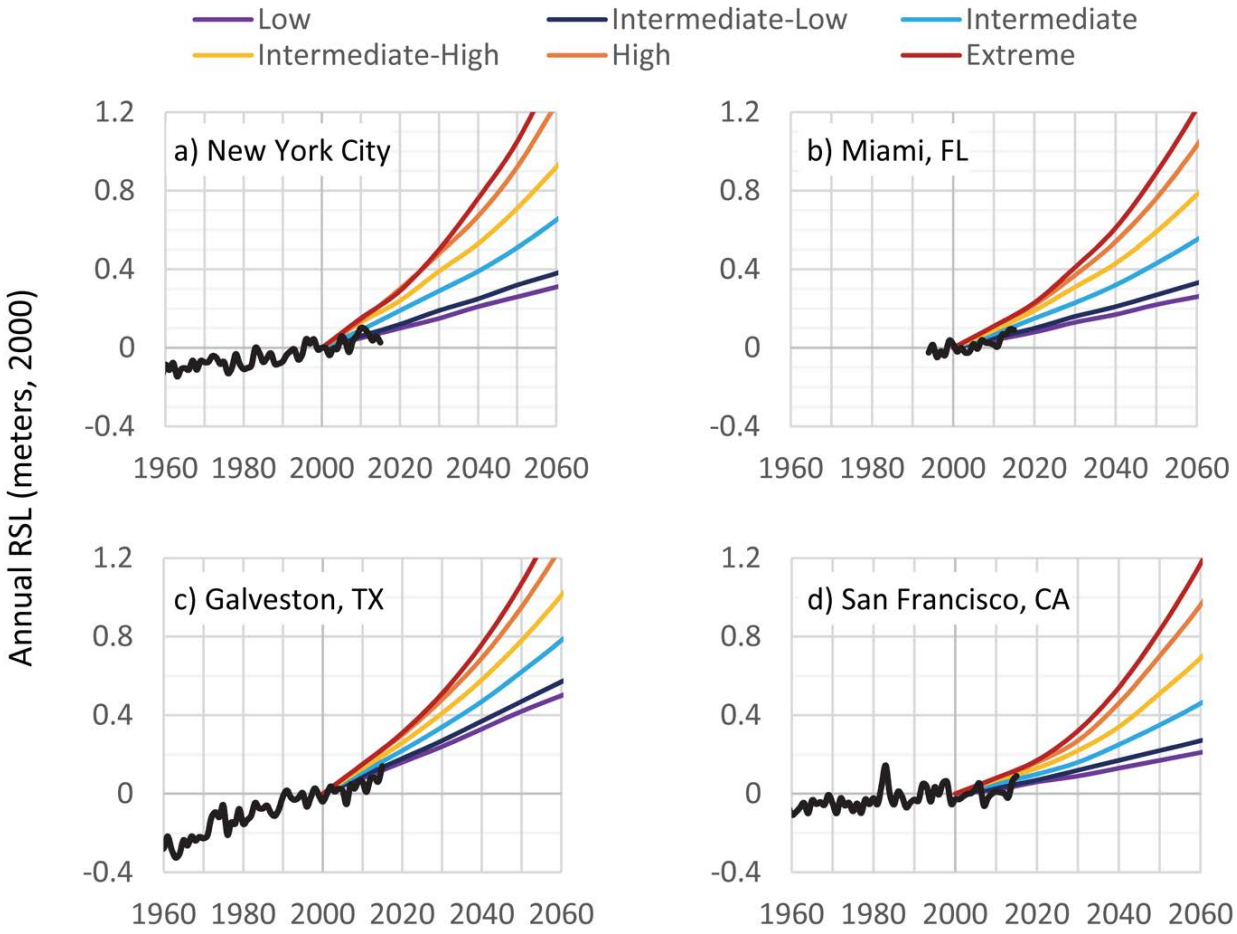

Figure 14. Average annual RSL for New York City (The Battery), Miami (Virginia Key), Fla., Galveston, Tex. and San Francisco, Calif. with their respective (median-value) RSL under the six scenarios. The NOAA RSL observations (tidesandcurrents.noaa.gov/sltrends) are shown relative to the midpoint (year 2000) of the 1991–2009 epoch (1994–2009 at Virginia Key), which is the reference level for the scenarios.

When planning under any sea level scenario, both short and/or long-term decisions should recognize that locations with lower elevation thresholds for impacts, less variability in extreme water levels, or higher rates of RSL rise have been the most prone to rapid (often-accelerating) increases in event probabilities (Sweet and Park, 2014) and will continue to be so in the future (Hunter, 2012; Tebaldi et al., 2012; Kopp et al., 2014, Sweet and Park, 2014; Buchanan et al., 2016). Return level interval curves of extreme water level events in New York City and San Francisco (Figure 15a, b) illustrate the differences in the extreme variance between locations (proportional to the gradient of the return level interval curve). As stated above, the focus here is on the higher probability (more frequent) events, which are better resolved statistically (i.e., tighter 95% confidence intervals) due to their more frequent nature than, for example, the extremely rare event such as associated with a hurricane landfall (Hall et al., 2016). Figure 15c shows the water level heights with a 20% annual chance of occurrence (5-year recurrence interval) for a set of NOAA tide gauges with more than 20 years of hourly observations. The 20% annual chance flood levels range from about 0.3 m (~1 foot), such as where narrow and deep continental shelves bathymetrically constrain the magnitude of storm surges (e.g., along the West Coast and Islands where wave runup and/or dynamic water levels [Stockdon et al., 2006; Sweet et al., 2015] can be larger than storm surge [Hoeke et al., 2013; Ruggiero, 2013; Serafin and Ruggiero, 2014]) to 0.9 m or more at higher latitudes, where powerful extratropical storms and wide continental shelves allow larger surges to build (Tebaldi et al., 2012; Hall et al., 2016; Merrifield et al., 2015, 2016). The median of the 20% annual chance flood in Figure 15c is about 0.8 m (ranging from about 0.3 m to

1.8 m) above MHHW, which is nearly the same as the National Weather Service's empirically derived elevations used to define 'moderate' flooding at dozens of NOAA tide gauges (~0.8 m and ranging from about 0.5 m to 1.8 m; http://water.weather.gov/ahps). Moderate level flooding is disruptive to commerce and damaging to private and commercial property; when such coastal flooding is imminent or occurring, NOAA typically issues a coastal/lakeshore flood *warning* of a serious risk to life and property (NOAA, 2014). In contrast, the median nuisance flood threshold around the U.S., which is associated with minor coastal flooding and issuance of a coastal flood *advisory*, can be expected to occur about two times per year (0.5-year recurrence interval) and is about 0.5 m above MHHW (Sweet et al., 2014).

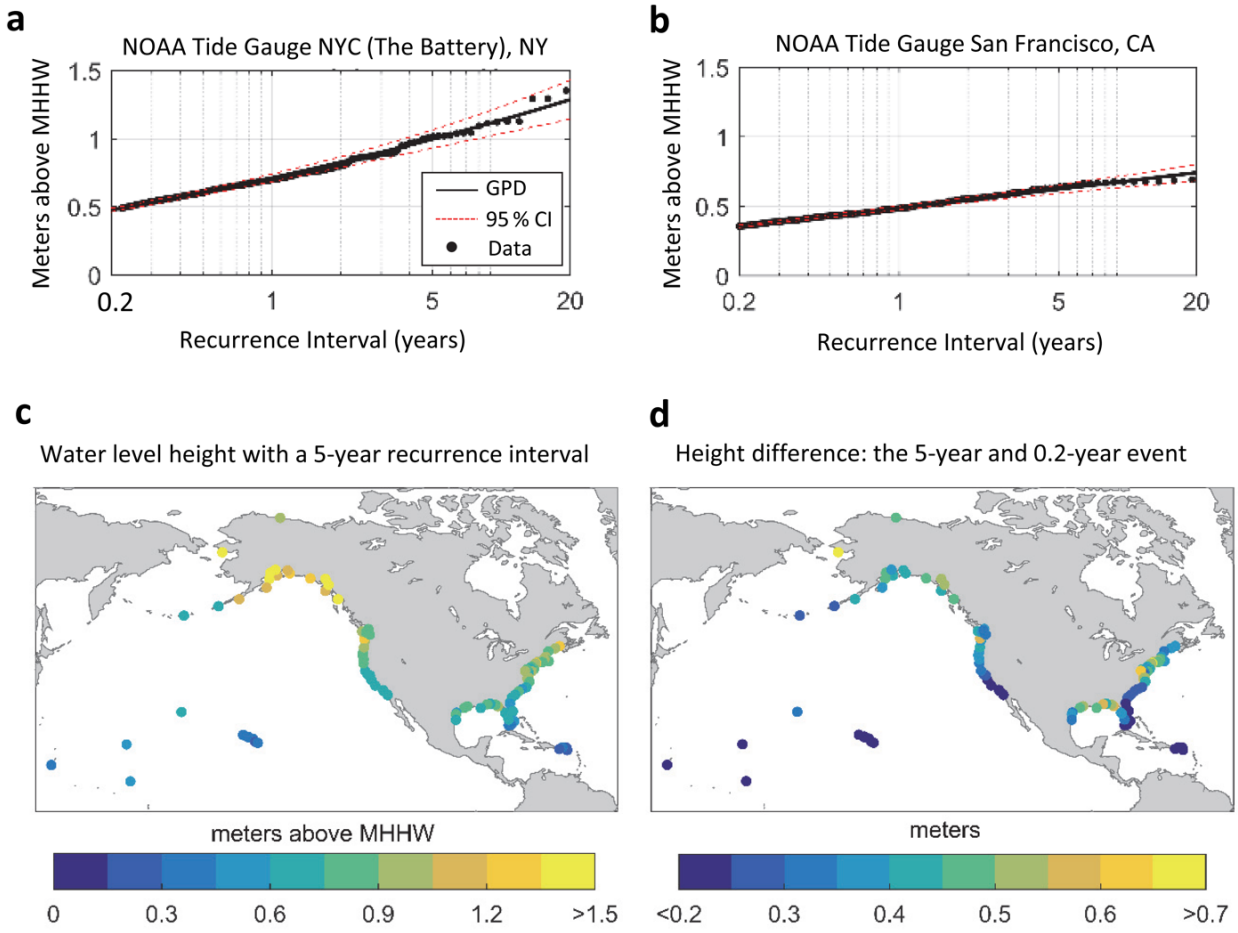

Figure 15. Generalized Pareto Distribution and 95% confidence interval (CI: red dash) fit for high-water extremes for historical data through 2015 (black dots) based upon Sweet et al. (2014) for NOAA tide gauges in a) New York City (The Battery), N.Y. and b) San Francisco, Calif. In c) is a map for water level heights (whose magnitudes are shown relative to the 1991–2009 epoch) with a 5-year recurrence interval (20% annual chance of occurrence) for a set of NOAA tide gauges with more than 20 years of hourly record [as in a) and b)], and d) shows the height difference between the water levels with a 5-year and a 0.2-year recurrence interval (happening five or more times per year).

Estimates of a location's high water distribution, which forms in response to high tides and storms, are needed to assess how and when flood frequencies are likely to change under future RSL rise. Figure 15d illustrates differences in water level heights associated for events with a 5-year (20% annual change event) and 0.2-year recurrence interval (happening five or more times per year), with the former representing disruptive/damaging flooding and the latter associated with localized shallow (more nuisance-like) tidal flooding. The height separating the two flood types provides a RSL rise-related 'time horizon' for a future when disruptive/damaging tidal flooding may become much more

commonplace (under current flood defenses). The median value in Figure 15d is about 0.35 m, with a range from about 0.1 m to 1.1 m. Thus, for most of U.S. tide gauge locations examined (108 locations; 90 along U.S. coastlines outside Alaska), with an additional 0.35-m rise (<14 in) in RSL, exposure to disruptive/damaging tidal flooding will become much more commonplace.

Figure 16 illustrates the decade when the 5-year event (20% annual chance) becomes a 0.2-year event—a 25-fold increase in event probability—from RSL rise under the low-to-moderate subset of the sea level scenarios (Low, Intermediate-Low, Intermediate and Intermediate-High). It is important to note that flooding during an event can span several high tides over the course of days (e.g., Sweet et al., 2016). Locations experiencing the most rapid increase in event probability in the coming decades in general have higher RSL rise and/or less extreme water-level variance (i.e., a smaller scale parameter—cf. Hunter, 2012 and Church et al., 2013a). Smaller variance in extreme event magnitudes, not surprisingly, is found within locations with typically calm condition (e.g., Florida Coast) and/or small storm surges (e.g., California and Pacific Island Coasts). These two parameters – magnitude of RSL rise and extreme water-level variance (independent variables) – largely explain the pattern of dates (dependent variable) shown in Figure 16 through a bivariate linear regression model (not shown; R^2 = 0.5, 0.6, 0.8 and 0.9 under the four scenarios shown, respectively). Considering RSL under the Low, Intermediate-Low, Intermediate and Intermediate-High scenarios (Figure 16a–d), disruptive/damaging tidal flooding will occur five or more times a year at most locations (90 cities) along the U.S. coastline (outside Alaska) by or about (±5 years) 2080, 2060, 2040 and 2030, respectively.

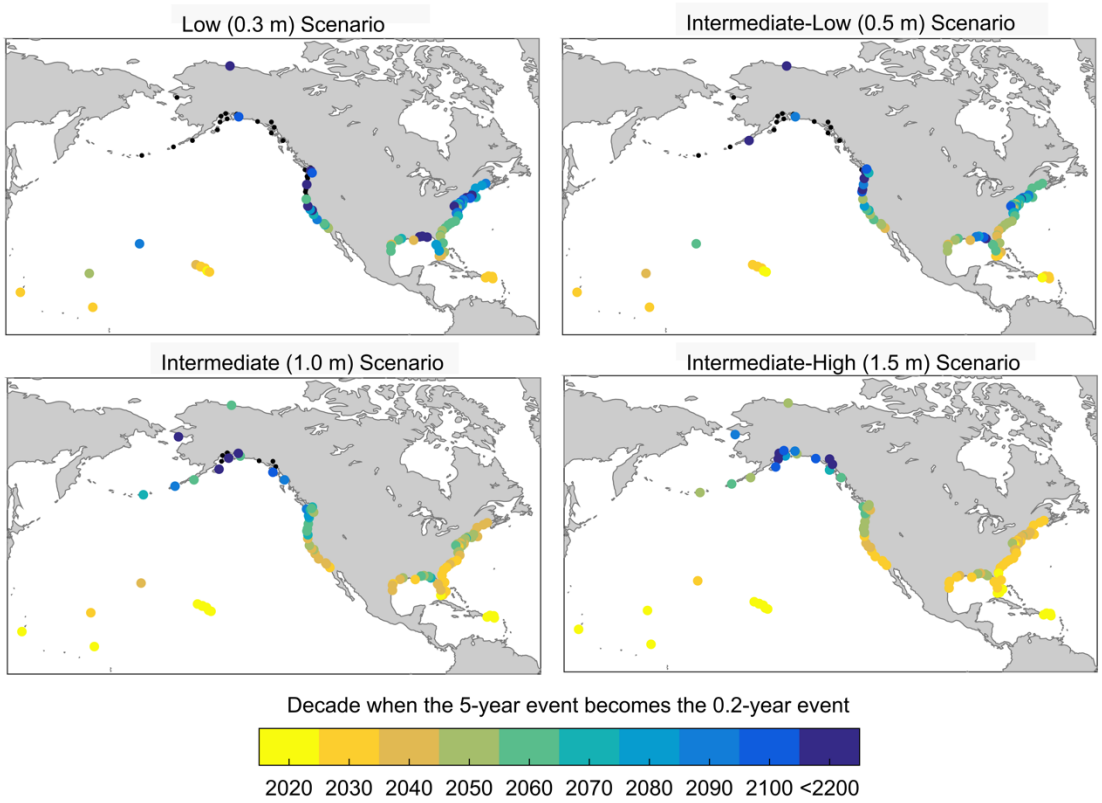

Figure 16. The decade (±5 years about the year shown in the legend) when the flood event with a 5-year recurrence interval (20% annual chance event) becomes a 0.2-year recurrence interval (or annual probability increases 25-fold) under location-specific RSL associated with the a) Low b) Intermediate-Low, c) Intermediate and d) Intermediate-High scenarios. Black dots are locations where the 5-year event does not transition to a 0.2-year event by 2200. Note: flooding during an event can occur at high tide for several days (e.g., Sweet et al., 2016).

6.3 Building for a Major Flood Event: A Case Study for South Florida

Consider a hypothetical flood risk-reduction structure needed by a community to reduce the flood risks associated with future RSL rise and its effects on extreme water level events. This example will use sea level scenarios for the region encompassing Key West, with probabilistic information on the extreme water levels estimated for its NOAA tide gauge as described for Figure 15. It is not intended to provide a detailed decision-making blueprint for a specific infrastructure facility; rather, this example illustrates the application of sea level scenarios and related changes in extreme water levels for decision-making. It also demonstrates how the previously described concepts of risk-based framing may be used to assist in determining design parameters for the structure.

The Florida Keys are well known to experience impacts from hurricane storm surges and from tidal flooding of streets and neighborhoods. Suppose that the region of Key West intends to plan, design, and construct a seawall using a 50-year period of economic analysis starting in 2020 and, as a consequence, the structure is expected to provide risk-reduction benefits for the period 2020 through 2070. Further suppose that the seawall is intended to protect against the 1% annual chance flood (i.e., with a 100-year recurrence interval) over this 50-year period. It is assumed that a community in the region would like to assume reasonably low levels of risks, and therefore, its practitioners have opted to use higher sea level rise scenarios as design criteria. In this specific example, two scenarios will be used as the design range. Using Table 4 as a guide, scenarios that have exceedance probabilities significantly lower than 50% are chosen, and thus the Intermediate (1.0-m) scenario is used as the lower bound for the design range. Based on the probabilistic analysis of Kopp et al. (2014), the exceedance probability for the corresponding GMSL is in the range of 2% to 17%. The Intermediate-High (1.5-m) scenario is chosen as the high end for the design range. Based on the probabilistic analysis of Kopp et al. (2014), the exceedance probabilities for these scenarios are in the range of 0.4% to 1.3% (Table 4). As noted previously, the GMSL exceedance probabilities for the scenarios may be underestimates due to effects such as Antarctic ice sheet instability. The corresponding low and high percentile RSL values (appendix C) also provide uncertainty bounds on RSL change (approximately 10^{th} to 90^{th} percentile) under a particular scenario. The Extreme (2.5-m) scenario, corresponding to about the 99.9^{th} percentile of GMSL (see Table 4), is also selected to represent a plausible worst-case scenario (least upper bound; Hinkel et al., 2015). This worst-case scenario can be used to assess the project performance under conditions of extreme RSL rise that are physically plausible but judged to have extremely low probabilities. Often, decision makers would like information on the performance of a structure in the event of what is currently believed to be a low-probability future, but one whose probability may be revised with additional scientific knowledge. RSL for the scenarios applicable for the Key West location are shown in Figure 17 (solid curves).

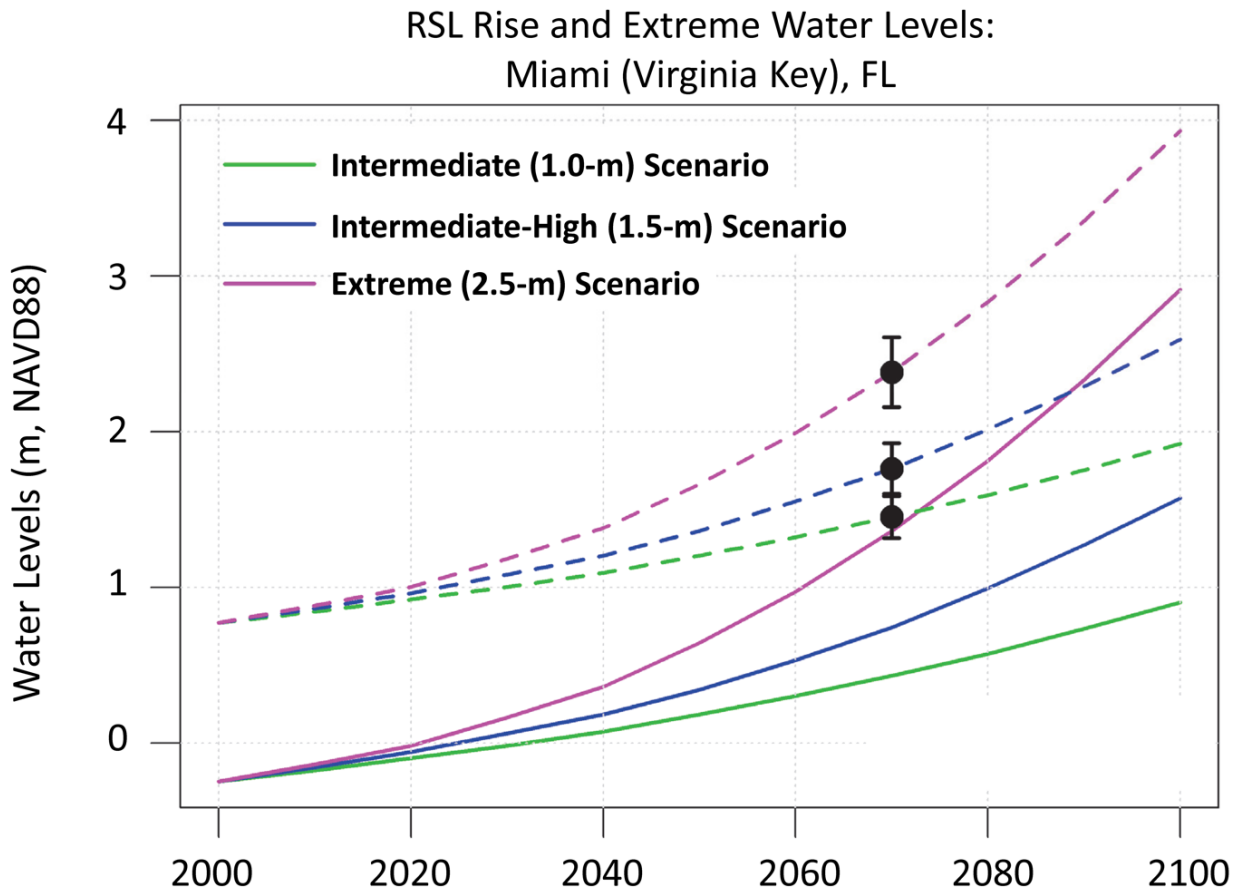

Figure 17. RSL under the Intermediate (1-m), Intermediate-High (1.5-m), and Extreme (2.5-m) GMSL rise scenarios (solid curves) for Florida Keys region, showing how the water level height with a 1% annual chance of occurring (dashed lines) and 95% confidence intervals (black error bars) estimated for year 2070 from hourly water levels at the NOAA Key West tide gauge changes in magnitude under each scenario. All curves have been expressed in terms of the geodetic datum NAVD88 using the tidal datums at Key West.

Practical use of RSL and extreme value projections, which typically reference NOAA's tidal datums, require an appropriate connection to a geodetic or map datum (e.g., NAVD88 or NGVD29). The RSL values shown in Figure 17 are referenced to NAVD88 (through its relationship to the 1983–2001 mean sea level datum using its local ~2.4 mm/year RSL trend). As was the approximation in Figure 17, it is assumed that the extreme value distribution is stationary except for its shifting upwards due to a change in mean sea level as prescribed by the scenario. The change in the 1% annual chance flood in response to increasing RSL under the various scenarios is shown in Figure 17 (dashed curves).

The uncertainty bounds on the projected 1% annual chance flood assume that RSL and the historical extremes are independent. The total uncertainty of the projected extremes is estimated by summing the computed variances of the individual RSL high and low percentile values (appendix C) and the estimated return level uncertainties (e.g., Figure 15a, b). The corresponding 95% confidence interval considering the uncertainty of both the RSL and the estimate of the extreme sea level is shown as error bars in Figure 17. A summary of results of the above calculations are shown in Table 7.

Table 7. RSL with 1% annual chance flood heights and confidence intervals (CI) over the 50-year economic period of analysis for Virginia Key, Fla. The RSL and extreme sea levels are relative to the geodetic datum NAVD88, which is 0.27 cm above local mean sea level for the 1983–2001 epoch.

	Intermediate	Intermediate-High	Extreme
GMSL rise between 2000 and 2100	1.0 m	1.5 m	2.5 m
Median RSL (Key West) in 2070	0.43 m (0.68 m rise since 2000)	0.76 m (1.01 m rise since 2000)	1.38 m (1.63 m rise since 2000)
1% annual chance flood	1.33 m	1.66 m	2.28 m
1% annual chance flood (5% CI)	1.16 m	1.41 m	1.88 m
1% annual chance flood (95% CI)	1.51 m	1.91 m	2.69 m

For the Intermediate scenario, the 1% annual chance flood (in meters NAVD88) and the corresponding 95% confidence interval is estimated to be 1.33 m (1.16 m, 1.51m), and the same for the Intermediate-High scenarios is 1.66 m (1.41 m, 1.91 m). Depending on risk tolerance, the practitioner may choose a value between these ranges for design. In addition, the last column provides information using the Extreme scenario (2.5 m GMSL rise by 2100), which will allow the practitioner to assess the consequences of a low-probability, but high-consequence scenario. For this Extreme scenario, the 1% annual chance flood could be as high as 2.28 m (1.88 m, 2.69 m). The decision to use the 1% annual chance flood at the end of the planning horizon (2070 in this case) will provide a higher level of risk-reduction benefits throughout the life of the project. Alternative approaches for risk-based design under nonstationarity are available, and they may provide design criteria that are either more or less stringent and costly (Salas and Obeysekera, 2014; Rootzen and Katz, 2013; Obeysekera and Salas, 2016; Buchanan et al. 2016). It is important to note that that the decision to reduce risks for longer engineering design periods or higher water levels entails additional cost. However, it is also true that, even if changes in RSL over the chosen time frame are lower than the optimized level of risk-reduction benefits selected, a high threshold selection can confer additional benefits, such as added risk reduction for larger storm surges (whether due to stronger storms with climate change, or natural variability), or risk-reduction benefits that extend beyond the period of economic analysis (just as infrastructure often provides benefits well beyond its intended design life).

7.0 SUMMARY AND NEXT STEPS

This technical report provides results and discussion related to two primary tasks: 1) developing an updated scenario range for possible 21st century GMSL rise and 2) producing a set of gridded RSL response along the United States coastline based on discrete scenarios drawn from this updated GMSL rise range. For the first task, we assessed recent observational and modeling literature on worst-case GMSL projections. Several studies argue for physically plausible GMSL rise in the range of 2.0–2.7 m, and recent results regarding Antarctic ice-sheet instability indicate that such outcomes may be more likely than previously thought. As such, this report recommends a range of GMSL rise of 0.3–2.5 m possible during the 21st century, which was previously reported as 0.2–2.0 m in Parris et al. (2012). The upward revision to the low-end GMSL rise scenario is based upon tide gauge and altimeter-based estimates of the rates of GMSL change over the past quarter-century and of recent modeling of future low-end projections of GMSL rise.

From this revised range for GMSL rise, RSL is projected on a 1-degree grid (and for precise locations of tide gauges) covering the U.S. mainland coastline, Alaska, Hawaii, the Caribbean, and the Pacific island territories for six representative GMSL rise scenarios by 2100: a Low, Intermediate-Low, Intermediate, Intermediate-High, High, and Extreme, which correspond to GMSL rise of 0.3, 0.5, 1.0, 1.5, 2.0 and 2.5 m, respectively. In recognition of long-term GMSL rise commitment (lagged GMSL response), GMSL and associated RSL values are quantified from the year 2000 through the year 2200 (on a decadal basis to 2100 and with lower temporal frequency between 2100 and 2200). The GMSL rise scenarios at each grid cell are adjusted to account for key factors important at regional scales, including 1) shifts in oceanographic factors such as circulation patterns; 2) changes in the Earth's gravitational field and rotation, and the flexure of its crust and upper mantle due to melting of land-based ice; and 3) VLM—subsidence or uplift—due to GIA (which also changes the shape of the ocean basin and sea level), sediment compaction, groundwater and fossil fuel withdrawals, and other nonclimatic factors. Key findings include that:

- For almost all future GMSL rise scenarios, RSL rise is projected to be greater than the global average along the coasts of the U.S. Northeast and the western Gulf of Mexico.
- Under the Intermediate and Low GMSL rise scenarios, RSL is projected to be less than the global average along much of the Pacific Northwest and Alaska coasts.
- Under the Intermediate-High, High and Extreme GMSL rise scenarios, RSL is projected to be higher than the global average along almost all U.S. coasts outside Alaska.

This 1-degree gridded set of scenario-based RSL projections for the U.S. is a new data product intended to fill a major gap in climate information needed to support a wide range of coastal assessment, planning, and decision-making processes. The gridded set provides scenario estimates of future RSL rise (and potential impacts) for locations within an individual grid, though it is recognized that local VLM may spatially deviate over 1 km to 10 km in some regions. By separating the climatic from the nonclimatic RSL contributions inherent to the RSL response under the scenarios, practitioners can modify the nonclimatic background rates accordingly (e.g., if anthropogenic forcing of VLM is thought to vary over the century). Systematic GMSL and RSL assessments will continue to refine the scenarios per contemporary scientific understanding of the processes contributing to extreme and rapid sea level change. Important to estimates of the probability of the higher-end scenarios (though not factored into the probability estimates included in this report or yet available in the peer-reviewed literature) are contributions from ice-cliff and ice-shelf feedback processes that may

significantly increase ice-sheet contributions to GMSL rise, particularly under high emissions scenarios (DeConto and Pollard, 2016).

This report draws attention to the consequences of RSL rise, which are already occurring. For example, tidal-flood frequencies for minor (nuisance) impacts are rapidly increasing and accelerating in dozens of coastal communities (Ezer and Atkinson, 2014; Sweet et al., 2014; Sweet and Park, 2014). We provide a broad assessment in terms of how continued RSL rise in the future under the sea level scenarios may affect the frequency of more significant moderate flooding, which impacts property, public services and commerce and is often associated with a NOAA coastal/lakeshore flood *warning*. The elevation threshold used to classify such events by NOAA on their tide gauges varies along the U.S. coastline, but in general it is about 0.8 m (2.6 feet) above the highest average tide and locally has a 20% annual chance of occurrence. Using this flood-frequency definition, we find at most locations examined (90 cities along the U.S. coastline outside of Alaska) that with only about 0.35 m (<14 in) of local RSL rise, annual frequencies of such disruptive/damaging flooding will increase 25-fold by or about (±5 years) 2080, 2060, 2040 and 2030 under the Low, Intermediate-Low, Intermediate, and Intermediate High subset of scenarios, respectively.

The GMSL and RSL products developed here will be a key input into the USGCRP Sustained Assessment process and inform the upcoming NCA4 due in 2018. They will also support the next steps of the Interagency Sea Level Rise and Coastal Flood Hazard Scenarios and Tools Task Force. These next steps will focus on the integration of these global and regional scenario products within the diversity of coastal risk management tools and capabilities deployed by individual agencies in support of the needs of specific stakeholder groups and user communities. This deployment of scenarios and tools will help serve as a starting point for on-the-ground coastal preparedness planning and risk management processes needed to ensure that U.S. coastal communities (and their economies) remain vibrant and resilient to ongoing and future changes in sea level.

ACKNOWLEDGEMENTS

We thank Ashley Miller of NOAA's Center for Operational Oceanographic Products and Services (CO-OPS) and Daniel Bader of the Center for Climate Systems Research at Columbia University for their help in data processing. We also thank Dr. John Hall, Director, Joint Fire Science Program (formerly with DoD SERDP/ESTCP), Dr. R. Steven Nerem of the University of Colorado, Lisa Auermuller of the Jacques Cousteau National Estuarine Research Reserve, Dr. Marissa Liang of the U.S. Environmental Protection Agency, and Dr. Greg Dusek, Senior Scientist of NOAA CO-OPS for their reviews* of this manuscript and constructive comments (*a review does not necessarily indicate agreement on all points of the final version).

We acknowledge the World Climate Research Programme's Working Group on Coupled Modeling, which is responsible for CMIP, and we thank the climate modeling groups (listed in appendix D) for producing and making available their model output. For CMIP, the U.S. Department of Energy's Program for Climate Model Diagnosis and Intercomparison provides coordinating support and led development of software infrastructure in partnership with the Global Organization for Earth System Science Portals.

REFERENCES

Bamber, J. and R. Riva (2010). The Sea Level Fingerprint of Recent Ice Mass Fluxes. The Cryosphere 4:621–627.

Bamber, J. L., and W. P. Aspinall (2013). An expert judgement assessment of future sea level rise from the ice sheets, Nat. Clim. Change, 3, 424–427, doi:10.1038/nclimate1778.

Boening, C., J. K. Willis, F. W. Landerer, R. S. Nerem, and J. Fasullo (2012). The 2011 La Niña: So strong, the oceans fell. Geophys. Res. Lett., 39, L19602, doi:10.1029/2012GL053055.

Boon, J. D., Brubaker, J. M. & Forrest, D. R. Chesapeake Bay Land Subsidence and Sea Level Change (2010). An Evaluation of Past and Present Trends and Future Outlook Special Report No. 425 in Applied Marine Science and Ocean Engineering (Virginia Institute of Marine Science, 2010).

Bromirski, P. D., Miller, A. J., Flick, R. E., & Auad, G. (2011). Dynamical suppression of sea level rise along the Pacific coast of North America: Indications for imminent acceleration. Journal of Geophysical Research: Oceans, 116(C7).

Buchanan, M.K., R.E. Kopp, M. Oppenheimer, C. Tebaldi (2016). Allowances for evolving coastal flood risk under uncertain local sea-level rise. Climatic Change. doi:10.1007/s10584-016-1664-7

Cazenave, A., H.-B. Dieng, B. Meyssignac, K. von Schuckmann, B. Descharme, and E. Berthier (2014). The rate of sea-level rise. Nat. Climate Change, 4, 358–361, doi:10.1038/nclimate2159.

Chambers, D. P., Cazenave, A., Champollion, N., Dieng, H., Llovel, W., Forsberg, R., ... & Wada, Y. (2016). Evaluation of the Global Mean Sea Level Budget between 1993 and 2014. Surveys in Geophysics, 1-19.

Church J.A., White N.J., Coleman R., Lambeck K., Mitrovica J.X. (2004) Estimates of the regional distribution of sea-level rise over the 1950 to 2000 period. J. Clim. 17:2609–2625.

Church, J. A., & White, N. J. (2011). Sea-level rise from the late 19th to the early 21st century. Surveys in *Geophysics*, *32*(4-5), 585-602.

Church, J. A and coauthors (2013a). Sea level change. Chapter 13 in Climate Change 2013: The Physical Science Basis. Contribution of Working Group I to the Fifth Assessment Report of the Intergovernmental Panel on Climate Change, Cambridge University Press, Cambridge, United Kingdom and New York, NY, USA, 1535.

Church, J. A. and coauthors (2013b). Sea-level rise by 2100. Science, 342(6165), 1445.

DeConto, R. M. and Pollard, D. (2016). Contribution of Antarctica to past and future sea-level rise. Nature, 531(7596), 591-597.

Deschamps, P., N. Durand, E. Bard, B. Hamelin, G. Camoin, A. L. Thomas, G. M. Henderson, J. Okuno, and Y. Yokoyama (2012). Ice-sheet collapse and sea-level rise at the Bølling warming 14,600 years ago, Nature, 483, 559–564, doi:10.1038/nature10902.

Eggleston, J. and J. Pope (2013). Land subsidence and relative sea-level rise in the southern Chesapeake Bay region: U.S. Geological Survey Circular 1392, 30 p., http://dx.doi.org/10.3133/cir1392.

Ezer, T. (2013). Sea level rise, spatially uneven and temporally unsteady: Why the US East Coast, the global tide gauge record, and the global altimeter data show different trends. Geophysical Research Letters, 40(20), 5439-5444.

Ezer, T. and L.P. Atkinson (2014). Accelerated flooding along the U.S. East Coast: on the impact of sea-level rise, tides, storms, the Gulf Stream, and the North Atlantic Oscillations. Earth's Future.2, 362-382. doi:10.1002/2014EF000252.

Fasullo, J. T., C. Boening, F. W. Landerer, and R. S. Nerem (2013). Australia's unique influence on global sea level in 2010–2011. Geophys. Res. Lett., 40, 4368–4373, doi:10.1002/grl.50834.

Firing, Y., M.A. Merrifield, T.A. Schroeder, and B. Qiu (2004). Interdecadal Sea Level Fluctuations at Hawaii. J. Phys. Oceanogr., 34, 2514–2524, doi: 10.1175/JPO2636.1.

Galloway, D.L., D.R. Jones, and S.E. Ingebritsen (1999). Land subsidence in the United States: U.S. Geological Survey Circular 1182, 175 p.

Goddard, P. B., J. Yin, S.M. Griffies, S. Zhang (2015). An extreme event of sea-level rise along the Northeast coast of North America in 2009–2010. Nat. Commun. 6:6346 doi: 10.1038/ ncomms7346.

Golledge, N.R., D. E.Kowalewski, T.R. Naish, R.H. Levy, C.J. Fogwill, and E.G.W. Gasson, (2015). The multi-millennial Antarctic commitment to future sea-level rise: Nature, v. 526, no. 7573, p. 421-425, doi:10.1038/nature15706.

Grinsted, A., S. Jevrejeva, R.E.M. Riva, and D. Dahl-Jensen, (2015). Sea Level Rise Projections for Northern Europe under RCP 8.5. Climate Research 64:15–23.

Gutierrez, B.T., S.J. Williams, and E.R. Thieler, (2009). Ocean coasts. In: Coastal Sensitivity to Sea-Level Rise: A Focus on the Mid-Atlantic Region. A report by the U.S. Climate Change Science Program and the Subcommittee on Global Change Research. [J.G. Titus (coordinating lead author), K.E. Anderson, D.R. Cahoon, D.B. Gesch, S.K. Gill, B.T. Gutierrez, E.R. Thieler, and S.J. Williams (lead authors)]. U.S. Environmental Protection Agency, Washington DC, pp. 43-56.

Hall, J.A., S. Gill, J. Obeysekera, W. Sweet, K. Knuuti, and J. Marburger (2016). Regional Sea Level Scenarios for Coastal Risk Management: Managing the Uncertainty of Future Sea Level Change and Extreme Water Levels for Department of Defense Coastal Sites Worldwide. U.S. Department of Defense, Strategic Environmental Research and Development Program. 224 pp.

Hallegatte, S., A. Shah, R. Lempert, C. Brown, and S. Gill. (2012). Investment Decision Making Under Deep Uncertainty – Application to Climate Change. World Bank Policy Research Working Paper 6193. World Bank, Washington, DC, USA.

Hamlington, B. D., R. R. Leben, K.-Y. Kim, R. S. Nerem, L. P. Atkinson, and P. R. Thompson (2015). The effect of the El Niño-Southern Oscillation on U.S. regional and coastal sea level, J. Geophys. Res. Oceans, 120, 3970–3986, doi:10.1002/2014JC010602.

Hamlington, B. D., R. R. Leben, M. W. Strassburg, R. S. Nerem, and K.-Y. Kim (2013). Contribution of the Pacific decadal oscillation to global mean sea level trends. Geophys. Res. Lett., 40, 5171–5175, doi:10.1002/grl.50950.

Hamlington, B. D., S. H. Cheon, P. R. Thompson, M. A. Merrifield, R. S. Nerem, R. R. Leben, and K.-Y. Kim (2016). An ongoing shift in Pacific Ocean sea level, J. Geophys. Res. Oceans, 121, 5084–5097, doi:10.1002/2016JC011815.

Hauer, M. E., J. M. Evans, and D R. Mishra (2016). Millions projected to be at risk from sea-level rise in the continental United States. Nature Climate Change.

Hay, C. C., Morrow, E., Kopp, R. E., & Mitrovica, J. X. (2015). Probabilistic reanalysis of twentieth-century sea-level rise. Nature, 517(7535), 481-484.

Hinkel, J., C. Jaeger, R.J. Nicholls, J. Lowe, O. Renn, and S. Peijun, (2015). Sea-level rise scenarios and coastal risk management. Nature Climate Change, 5, 188-190.

Hoeke, R. K., K. L. McInnes, J. C. Kruger, R.J. McNaught, J. R. Hunter, and S. G. Smithers (2013), Widespread inundation of Pacific islands triggered by distant-source wind-waves, Glob. Planet. Chang.,108, 128–138, doi:10.1016/j.gloplacha.2013.06.006.

Horton, R., C. Herweijer, C. Rosenzweig, J. Liu, V. Gornitz and A.C. Ruane (2008). Sea level rise projections for current generation CGCMs based on the semi-empirical method, Geophys. Res. Lett., Vol. 35, L02715, doi: 10.1029/2007GL032486.

Horton, R.M., C. Little, V. Gornitz, D. Bader, and M. Oppenheimer (2015). Sea Level Rise and Coastal Storms. Annals of the New York Academy of Sciences 1336 (1), 36-44.

Hunter, J. (2012). A Simple Technique for Estimating an Allowance for Uncertain Sea-Level Rise. Clim. Chang. 113:239–252.

Intergovernmental Panel on Climate Change (2013). Summary for policymakers, in Climate Change 2013: The Physical Science Basis, edited by T. F. Stocker, D. Qin, G.-K. Plattner, M. Tignor, S. K. Allen, J. Boschung, A. Nauels, Y. Xia, V. Bex, and P. Midgley, pp. 3–29, Cambridge Univ. Press, Cambridge, U. K.

Jackson, L.P. and S. Jevrejeva. (2016). A probabilistic approach to 21st century regional sea-level projections using RCP and High-end scenarios. Global and Planetary Change, 146, pp.179-189.

Jevrejeva, S., A. Grinsted, & J.C. Moore. (2014). Upper limit for sea level projections by 2100. Environ. Res. Lett., 9(10), 104008.

Joughin, I., B.E. Smith, & B. Medley. (2014). Marine ice sheet collapse potentially under way for the Thwaites Glacier Basin, West Antarctica. Science, 344(6185), 735-738.

Kemp, A. C., B.P Horton, J.P. Donnelly, M.E. Mann, M. Vermeer, & S. Rahmstorf. (2011). Climate related sea-level variations over the past two millennia. Proceedings of the National Academy of Sciences, 108(27), 11017-11022.

Khan, N. S., E. Ashe, T.A. Shaw, M. Vacchi, J. Walker, W.R. Peltier, ... & B.P Horton. (2015). Holocene relative sea-level changes from near-, intermediate-, and far-field locations. Current Climate Change Reports, 1(4), 247-262.

Khan, S. A., K.H. Kjær, M. Bevis, J.L. Bamber, J. Wahr, K.K. Kjeldsen, ... & L. Liu. (2014). Sustained mass loss of the northeast Greenland ice sheet triggered by regional warming. Nature Climate Change, 4(4), 292-299.

King, D., D. Schrag, D. Zhou, Q. Ye, and A. Ghosh (2015). Climate Change: A Risk Assessment. University of Cambridge Centre for Science and Policy, 154 pp.

Kirwan, M.L., Guntenspergen, G.R., D'Alpaos, A., Morris, J.T., Mudd, S.M., and Temmerman, S. (2010). Limits on the adaptability of coastal marshes to rising sea level: Geophys. Res. Lett., v. 37, no. 23, p. L23401.

Kopp, R. E. (2013). Does the mid-Atlantic United States sea level acceleration hot spot reflect ocean dynamic variability?. Geophys. Res. Lett., 40(15), 3981-3985.

Kopp, R. E., C.C Hay, C.M Little, & J.X. Mitrovica. (2015). Geographic variability of sea-level change. Current Climate Change Reports, 1(3), 192-204.

Kopp, R. E., R.M. Horton, C.M. Little, J.X. Mitrovica, M. Oppenheimer, D.J. Rasmussen, B. Strauss, C. Tebaldi. (2014). Probabilistic 21st and 22nd century sea-level projections at a global network of tide-gauge sites. Earth's Future, 2(8), 383-406.

Kopp, R. E., A.C. Kemp, K. Bittermann, B.P Horton, J.P Donnelly, W.R. Gehrels, & S. Rahmstorf. (2016a). Temperature-driven global sea-level variability in the Common Era. Proceedings of the National Academy of Sciences, 201517056.

Kopp, R.E., A. Broccoli, B. Horton, D. Kreeger, R. Leichenko, J.A. Miller, J.K. Miller, P. Orton, A. Parris, D. Robinson, C.P. Weaver, M. Campo, M. Kaplan, M. Buchanan, J. Herb, L. Auermuller and C. Andrews. (2016b). Assessing New Jersey's Exposure to Sea-Level Rise and Coastal Storms: Report of the New Jersey Climate Adaptation Alliance Science and Technical Advisory Panel. Prepared for the New Jersey Climate Adaptation Alliance. New Brunswick, New Jersey.

Lempert, R. (2013). Scenarios that illuminate vulnerabilities and robust responses. Clim. Chang., 117:627-646.

Lentz, E., E.R. Thieler, N.G. Plant, S.R. Stippa, R.M. Horton, and D.B. Gesch (2016), Evaluation of dynamic coastal response to sea-level rise modifies inundation likelihood, Nat. Clim. Chang.

Leuliette, E. W. (2015). The balancing of the sea-level budget, Curr. Clim. Chang. Rep., 1, 3, 185–191, doi:10.1007/s40641-015-0012-8.

Leuliette, E.W., and R.S. Nerem (2016). Contributions of Greenland and Antarctica to global and regional sea level change. Oceanography 29(4):154–159, doi:10.5670/oceanog.2016.107

Levermann, A., P.U. Clark, B. Marzeion, G.A. Milne, D. Pollard, V. Radic, & A. Robinson. (2013). The multimillennial sea-level commitment of global warming. Proceedings of the National Academy of Sciences, 110(34), 13745-13750.

Marcos, M., F. M. Calafat, A. Berihuete, and S. Dangendorf (2015), Long-term variations in global sea level extremes, J. Geophys. Res. Oceans, 120, 8115– 8134, doi:10.1002/2015JC011173.

Martín-Español, A., A. Zammit-Mangion, P.J. Clarke, T. Flament, V. Helm, M.A. King, S.B. Luthcke, E. Petrie, F. Rémy, N. Schön. and B. Wouters (2016). Spatial and temporal Antarctic Ice Sheet mass trends, glacio-isostatic adjustment, and surface processes from a joint inversion of satellite altimeter, gravity, and GPS data. J. of Geophys. Res.: Earth Surface.

Marzeion, B., A. H. Jarosch, and M. Hofer (2012), Past and future sea-level change from the surface mass balance of glaciers, Cryosphere, 6, 1295–1322, doi:10.5194/tc-6-1295-2012.

Masterson, J.P., Fienen, M.N., Thieler, E.R., Gesch, D.B., Gutierrez, B.T., and Plant, N.G. (2014). Effects of sea-level rise on barrier island groundwater system dynamics – ecohydrological implications: Ecohydrol., v. 7, no. 3, p. 1064-1071.

Melillo, J. M., T.C. Richmond and G. W. Yohe, Eds. (2014). Climate Change Impacts in the United States: The Third National Climate Assessment. U.S. Global Change Research Program, 841 pp. doi:10.7930/J0Z31WJ2.

Menéndez, P.L Woodworth (2010). Changes in extreme high water levels based on a quasi-global tide-gauge dataset. J. Geophys. Res. 115, C10011.doi: 10.1029/2009JC005997

Mengel, M., A. Levermann, K. Frieler, A. Robinson, B. Marzeion, & R. Winkelmann. (2016). Future sea level rise constrained by observations and long-term commitment. Proceedings of the National Academy of Sciences, 113(10), 2597-2602.

Merrifield, M. A., P. Thompson, and M. Lander (2012), Multidecadal sea level anomalies and trends in the western tropical Pacific, Geophys. Res. Lett., 39, L13602, doi:10.1029/2012GL052032

Merrifield, M.A., E. Leuliette, P. Thompson, D. Chambers, B. D. Hamlington, S. Jevrejeva, J. J. Marra, M. Menéndez, G. T. Mitchum, R. S. Nerem, and W. Sweet (2016). [Global oceans] Sea level variability and change [in "State of the Climate in 2015"]. Bull. Amer. Meteor. Soc.

Merrifield, M.A., P. Thompson, E. Leuliette, G. T. Mitchum, D. P. Chambers, S. Jevrejeva, R. S. Nerem, M. Menéndez, W. Sweet, B. Hamlington, J. J. Marra (2015). [Global oceans] Sea level variability and change [in "State of the Climate in 2014"]. Bull. Amer. Meteor. Soc.

Miller, K. G., R. E. Kopp, B. P. Horton, J. V. Browning, and A. C. Kemp (2013), A geological perspective on sea-level rise and impacts along the U.S. mid-Atlantic coast, Earth's Future, 1, 3–18, doi:10.1002/2013EF000135.

Mitrovica, J. X., N. Gomez, E. Morrow, C. Hay, K. Latychev, and M. E. Tamisiea (2011). On the robustness of predictions of sea level fingerprints, Geophys. J. Int., 187(2), 729–742, doi:10.1111/j.1365-246X.2011.05090.x.

Nerem, R. S., D. Chambers, C. Choe, and G. T. Mitchum (2010). Estimating Mean Sea Level Change from the TOPEX and Jason Altimeter Missions. Mar. Geod., 33, 435–446, doi:10.1080/01490419.2010.4910.

National Research Council (2009). Informing Decisions in a Changing Climate. Panel on Strategies and Methods for Climate-Related Decision Support, Committee on the Human Dimensions of Global Change. Division of Behavioral and Social Sciences and Education. Washington, DC: The National Academies Press.

National Research Council (2012). Sea-Level Rise for the Coasts of California, Oregon, and Washington: Past, Present, and Future. Washington, D.C.: The National Academies Press. http://www.nap.edu/openbook.php?record_id=13389

NOAA (2003). Computational Techniques for Tidal Datums Handbook. NOAA Special Publication NOS CO-OPS 2. Silver Spring, Maryland: U.S. Department of Commerce, NOAA, National Ocean Service, Center for Operational Oceanographic Products and Services.

NOAA (2014). National Weather Service Instruction 10-320. Surf Zone Forecast & Coastal/Lakeshore Hazard Services. http://www.nws.noaa.gov/directives/sym/pd01003020curr.pdf

Obeysekera, J. and J.D. Salas (2016). Frequency of Recurrent Extreme Events under Nonstationarity. J. Hydrol. Engr., pub. Online Feb. 2016, ASCE, ISSN 1084-0699.

Oppenheimer, M., and R.B. Alley (2016). How high will the seas rise? Science, 354, 1375-1377.

Park J., J. Obeysekera, J. Barnes. (2010). Temporal Energy Partitions of Florida Extreme Sea Level Events as a function of Atlantic Multidecadal Oscillation, Ocean Sci., 6, 587-593.

Park, J., and W. Sweet. (2015). Accelerated sea level rise and Florida current transport. Ocean Sci. 11, 607–615, doi:10.5194/os-11-607-2015.

Parris, A., P. Bromirski, V. Burkett, D. Cayan, M. Culver, J. Hall, R. Horton, K. Knuuti, R. Moss, J. Obeysekera, A. Sallenger, and J. Weiss (2012). Global Sea Level Rise Scenarios for the US National Climate Assessment. NOAA Tech Memo OAR CPO-1. 37 pp.

Peltier, W. R. (2004). Global glacial isostasy and the surface of the ice-age Earth: the ICE-5G (VM2) model and GRACE. Annu. Rev. Earth Planet. Sci., 32, 111-149.

Perrette, M., F. Landerer, R. Riva, K. Frieler, and M. Meinshausen. (2013). A Scaling Approach to Project Regional Sea Level Rise and Its Uncertainties. Earth System Dynamics 4:11–29.

Pfeffer, W. T., Harper, J. T. and O'Neel, S. (2008). Kinematic constraints on glacier contributions to 21st-century sea-level rise. Science, 321(5894), 1340-1343.

Pollard, D., R.M. DeConto, & R.B. Alley. (2015). Potential Antarctic Ice Sheet retreat driven by hydrofracturing and ice cliff failure. Earth Planet. Sci. Lett., 412, 112-121.

Rahmstorf, S., J.E. Box, G. Feulner, M.E. Mann, A. Robinson, S. Rutherford, and E.J. Schaffernicht, (2015). Exceptional twentieth-century slowdown in Atlantic Ocean overturning circulation, Nat. Clim. Chang., vol. 5, pp. 475-480.

Rahmstorf, S. (2007). A Semi-Empirical Approach to Projecting Future Sea-Level Rise, Science Vol. 315

Ranger, N., T. Reeder, and J. Lowe (2013). Addressing 'deep' uncertainty over long-term climate in major infrastructure projects: four innovations of the Thames Estuary 2100 Project. European Journal on Decision Processes, 1, 233–262. doi:10.1007/s40070-013-0014-5.

Rignot, E., Mouginot, J., Morlighem, M., Seroussi, H., & Scheuchl, B. (2014). Widespread, rapid grounding line retreat of Pine Island, Thwaites, Smith, and Kohler glaciers, West Antarctica, from 1992 to 2011. Geophys. Res. Lett., 41(10), 3502-3509.

Rohling, E. J., I. D. Haigh, G. L. Foster, A. P. Roberts, and K. M. Grant (2013). A geological perspective on potential future sea-level rise, Nat. Sci. Rep., 3, 3461, doi:10.1038/srep03461.

Rootzen, H. and R.W. Katz (2013). Design Life Level: Quantifying Risk in a Changing Climate. Water Resour. Res., 49, 5964-5972, doi:10.1002/wrcr.20425

Ruggiero, P. (2013). Is the intensifying wave climate of the US Pacific northwest increasing flooding and erosion risk faster than sea-level rise?. J. Waterway Port Coastal Ocean Eng., 139(2), 88–97.

Salas, J.D. and J. Obeysekera (2014). Revisiting the Concepts of Return Period and Risk for Nonstationary Hydrologic Extreme Events. ASCE J. Hydrol. Engr., 19(3), 554-568.

Sato, T., C. Larsen, S. Miura, Y. Ohta, H. Fujimoto, W. Sun, R. Motyka, and J. Freymueller (2011). Reevaluation of the viscoelastic and elastic responses to the past and present–day ice changes in Southeast Alaska, Tectonophysics, 511, 79–88, doi:10.1016/j.tecto.2010.05.009.

Scambos, T., and C. Shuman, (2016). Comment on 'Mass gains of the Antarctic ice sheet exceed losses' by HJ Zwally and others. J. Glaciol.: 1-5.

Sella, G.F., S. Stein, T.H. Dixon, M. Craymer, S. James, S. Mazzotti. & R.K. Dokka, (2007). Observation of glacial isostatic adjustment in 'stable' North America with GPS. Geophys. Res. Lett., 34 (L02306), doi:10.10292006GL027081.

Seo, K.W., C.R. Wilson, T. Scambos, B.M. Kim, D.E. Waliser, B. Tian, B.H. Kim. and J. Eom. (2015). Surface mass balance contributions to acceleration of Antarctic ice mass loss during 2003–2013. J. Geophys. Res.: Solid Earth, 120(5), pp.3617-3627.

Serafin, K. A. and P. Ruggiero (2014). Simulating extreme total water levels using a time-dependent, extreme value approach. J. Geophys. Res. Oceans, 119, doi:10.1002/2014JC010093.

Shepherd, A., E. Ivins, G. Aa, V. Barletta, M. Bentley, S. Bettadpur…H.J. Zwally. (2012). A reconciled estimate of ice-sheet mass balance. Science, 338, 1183–1189.

Slangen, A. B. A., M. Carson, C.A. Katsman, R.S.W. van de Wal, A. Köhl, L.L.A. Vermeersen, & D. Stammer. (2014). Projecting twenty-first century regional sea-level changes. Climatic Change, 124(1-2), 317-332.

Stockdon, H.F., R.A. Holman, P.A. Howd, and A.H. Sallenger. (2006). Empirical Parameterization of Setup, Swash, and Runup. Coastal Engineering 53:573–588.

Sriver, R. L., N. M. Urban, R. Olson, and K. Keller. (2012). Toward a physically plausible upper bound of sea-level rise projections, Clim. Chang., 115, 893–902.

Sweet, W.V., C. Zervas, S. Gill, J. Park (2013). Hurricane Sandy Inundation Probabilities Today and Tomorrow [In "Explaining Extreme Events of 2012 from a Climatic Perspective"], Bull Amer. Meteor. Soc. 94 (9), S17–S20.

Sweet, W. V., J. Park, J. J. Marra, C. Zervas, and S. Gill (2014), Sea level rise and nuisance flood frequency changes around the United States, NOAA Tech. Rep. NOS CO-OPS 73, 53 pp.

Sweet, W.V. and J. Park (2014). From the extreme and the mean: Acceleration and tipping point of coastal inundation from sea level rise. Earth Futures, 2 579-600. DOI: 10.1002/2014EF000272

Sweet, W.V., J. Park, S. Gill, and J. Marra (2015). New Ways to Measure Waves and Their Effects at NOAA Tide Gauges: A Hawaiian-Network Perspective. Geophysical Research Letters 42:9355–9361. doi:10.1002/2015GL066030.

Sweet, W. V. and J. J. Marra, (2016). 2015 State of U.S. Nuisance Tidal Flooding. Supplement to State of the Climate: National Overview for May 2016, published online June 2016. http://www.ncdc.noaa.gov/monitoring-content/sotc/national/2016/may/sweet-marra-nuisance-flooding-2015.pdf

Sweet, W., M. Menendez, A. Genz, J. Obeysekera, J. Park, J. Marra (2016). In Tide's Way: Southeast Florida's September 2015 Sunny-day Flood [in "Explaining Extremes of 2015 from a Climate Perspective"]. Bull. Amer. Meteor. Soc., 97 (12), S25–S30, doi:10.1175/BAMS-D-16-0149.

Taylor, K. E., R. J. Stouffer, and G. A. Meehl (2012). An overview of CMIP5 and the experiment design, Bull. Amer. Meteor. Soc., 93(4), 485–498, doi:10.1175/BAMS-D-11-00094.1.

Tebaldi, C., B. H. Strauss, and C. E. Zervas. (2012): Modeling sea level rise impacts on storm surges along US coasts. Environ. Res. Lett., 7, 014032, doi:10.1088/1748-9326/7/1/014032.

Tedesco, M., Doherty, S., Fettweis, X., Alexander, P., Jeyaratnam, J., & Stroeve, J. (2016). The darkening of the Greenland ice sheet: trends, drivers, and projections (1981–2100). Cryosphere (The), 10, 477-496.

Theuerkauf, E. J., A. B. Rodriguez, S. R. Fegley, and R. A. Luettich Jr. (2014), Sea level anomalies exacerbate beach erosion, Geophys. Res. Lett., 41, 5139–5147, doi:10.1002/2014GL060544.

USACE. (2013). Incorporating Sea Level Change in Civil Works Programs. ER 1100-2-8162. Washington, D.C.: USACE.

USACE, (2014). Procedures to evaluate sea-level change: impacts, responses, and adaptation, U.S. Army Corps of Engineers, Technical Letter No. 1100-2-1, 254 p.

van Vuuren, D. P., J. Edmonds, M. Kainuma, K. Riahi, A. Thomson, K. Hibbard…S. Rose. (2011). The representative concentration pathways: An overview, Clim. Chang., 109, 5–31, doi:10.1007/s10584-011-0148-z.

Wahl, T. and D.P. Chambers. (2016). Climate controls multidecadal variability in U. S. extreme sea level records. J. Geophys. Res. 121.doi:10.1002/2015JC011057.

Weaver, C.P., R.J. Lempert, C. Brown, J.A. Hall, D. Revell, and D. Sarewitz, 2013: Improving the contribution of climate model information to decision-making: The value and demands of robust decision frameworks. Wiley Interdisciplinary Reviews Climate Change, 4, 39-60.

Weiss, J., J. Overpeck, and B. Strauss. (2011). Implications of recent sea level rise science for low-elevation areas in coastal cities of the conterminous U.S.A: Clim. Chang., v. 105, no. 3, p. 635-645.

White House, (2014). President's State, Local, and Tribal Leaders Task Force on Climate Preparedness and Resilience: Recommendations to the President. Washington, D.C., USA. https://www.whitehouse.gov/sites/default/files/docs/task_force_report_0.pdf.

Wong, P.P., I.J. Losada, J.-P. Gattuso, J. Hinkel, A. Khattabi, K.L. McInnes, Y. Saito, and A. Sallenger, (2014). Coastal systems and low-lying areas. In: Climate Change 2014: Impacts, Adaptation, and Vulnerability. Part A: Global and Sectoral Aspects. Contribution of Working Group II to the Fifth Assessment Report of the Intergovernmental Panel on Climate Change [Field, C.B., V.R. Barros, D.J. Dokken, K.J. Mach, M.D. Mastrandrea, T.E. Bilir, M. Chatterjee, K.L. Ebi, Y.O. Estrada, R.C. Genova, B. Girma, E.S. Kissel, A.N. Levy, S. MacCracken, P.R. Mastrandrea, and L.L.White (eds.)]. Cambridge University Press, Cambridge, United Kingdom and New York, NY, USA, pp. 361-409

Woodworth, P.L. and M. Menéndez. (2015). Changes in the mesoscale variability and in extreme sea levels over two decades as observed by satellite altimetry. J. Geophys. Res. 120, 64-77. doi:10.1002/2014jc010363

Yin, J. and P.B. Goddard. (2013). Oceanic control of sea level rise patterns along the East Coast of the United States. Geophys. Res. Lett., 40(20), 5514-5520.

Yin, J.J. (2012). Century to Multi-Century Sea Level Projections from CMIP5 Models. Geophys. Res. Lett. 39:L17709. doi:10.1029/2012GL052947.

Zervas, C. (2009). Sea Level Variations of the United States 1854–2006. NOAA Technical Report NOS CO-OPS 053, 75p, Appendices A–E.

Zervas, C., S. Gill, and W. V. Sweet (2013). Estimating vertical land motion from long-term tide gauge records, in NOAA Tech. Rep. NOS CO-OPS 65, 22 pp.

LIST OF APPENDICES

APPENDIX A. SEA LEVEL RISE AND COASTAL FLOOD HAZARD SCENARIOS AND TOOLS INTERAGENCY TASK FORCE

Convening organizations: The U.S. Global Change Research Program (USGCRP) and the National Ocean Council (NOC) at the request of the White House Council on Climate Preparedness and Resilience

Participating agencies: DoD, EPA, FEMA, NASA, NOAA, USACE, USGS

Membership:

Adrienne Antoine (NOAA)
Mark Crowell (FEMA)
John Haines (USGS, Co-Chair)
John Hall (DoD, former member; now BLM)
Radley Horton (Columbia University, NASA/GISS)
Paul Huang (FEMA)
Marissa Liang (EPA)
Carolyn Lindley (NOAA)
Kris Ludwig (USGS)
Audra Luscher (NOAA)
Doug Marcy (NOAA)
Heidi Moritz (USACE)
Rob Thieler (USGS)
Chris Weaver (EPA, Co-Chair)
Kate White (USACE)

APPENDIX B. LOW AND HIGH CLIMATE-RELATED RSL CHANGE CORRESPONDING TO GMSL SCENARIOS

The maps below show, for each GMSL scenario, the 17th and 83rd percentile of RSL change in 2100 (relative to 2000) among those samples from the probabilistic RSL distribution consistent with each GMSL scenario. They are presented relative to the median GMSL change for the scenario, as in Figure 9.

Low (0.3 m) GMSL Scenario

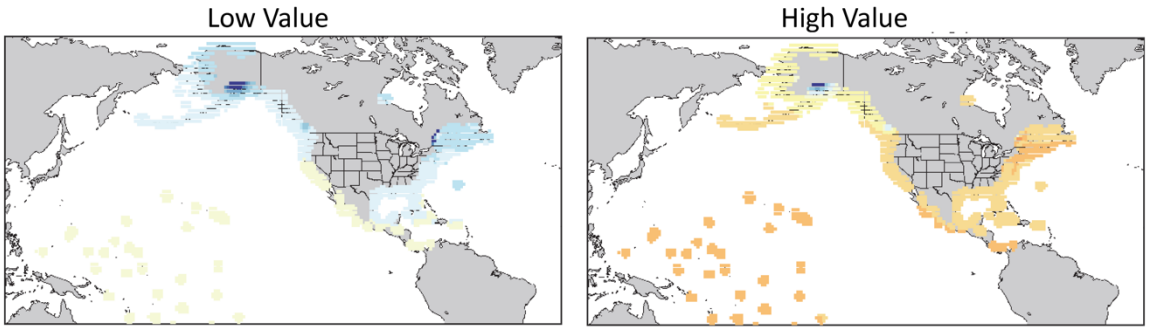

Intermediate-Low (0.5 m) GMSL Scenario

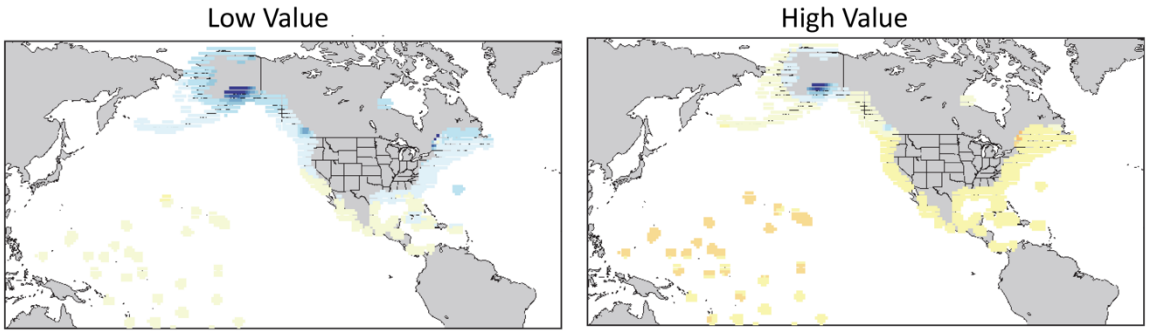

Intermediate (1.0 m) GMSL Scenario

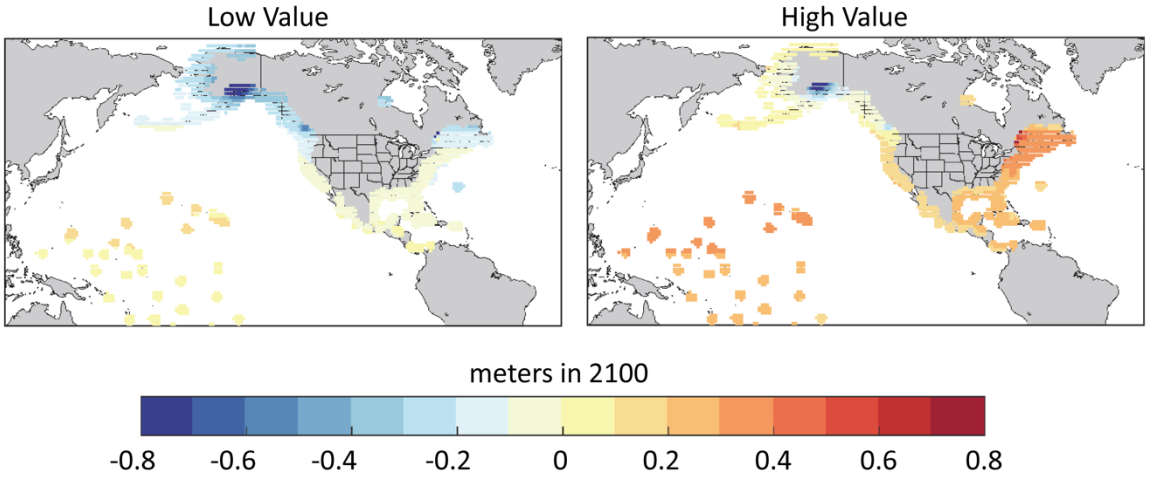

Appendix B: continued

Intermediate-High (1.5 m) GMSL Scenario

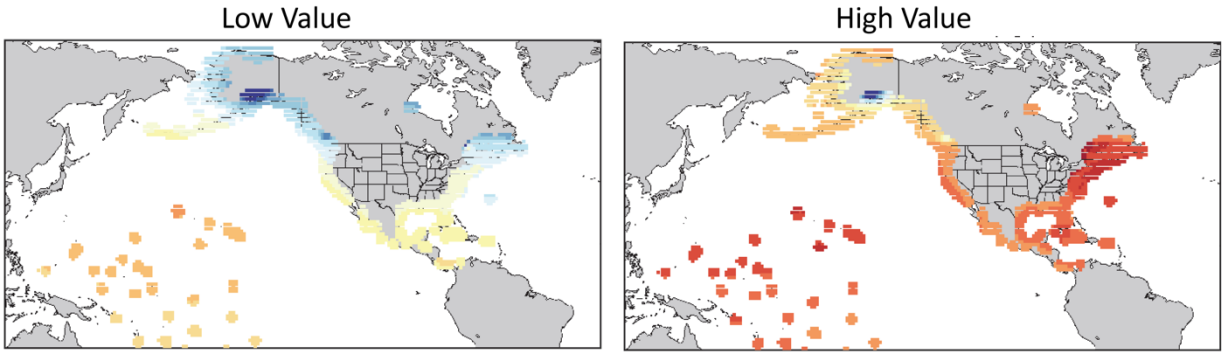

High (2.0 m) GMSL Scenario

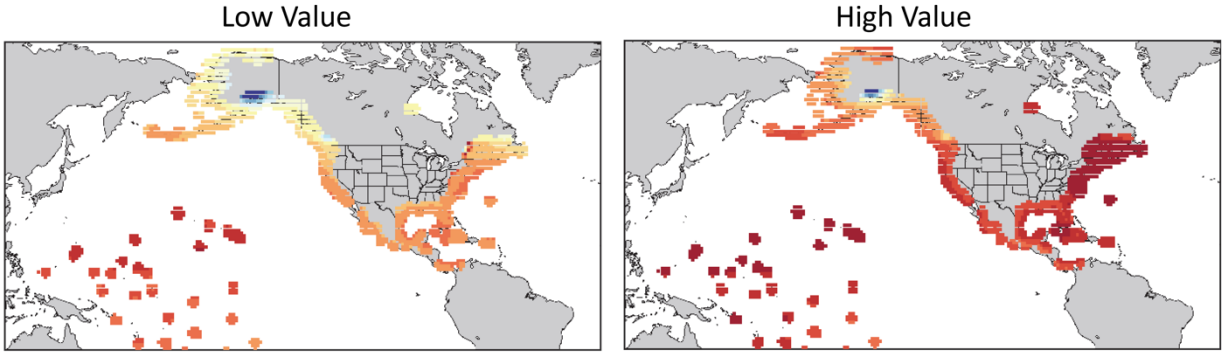

Extreme (2.5 m) GMSL Scenario

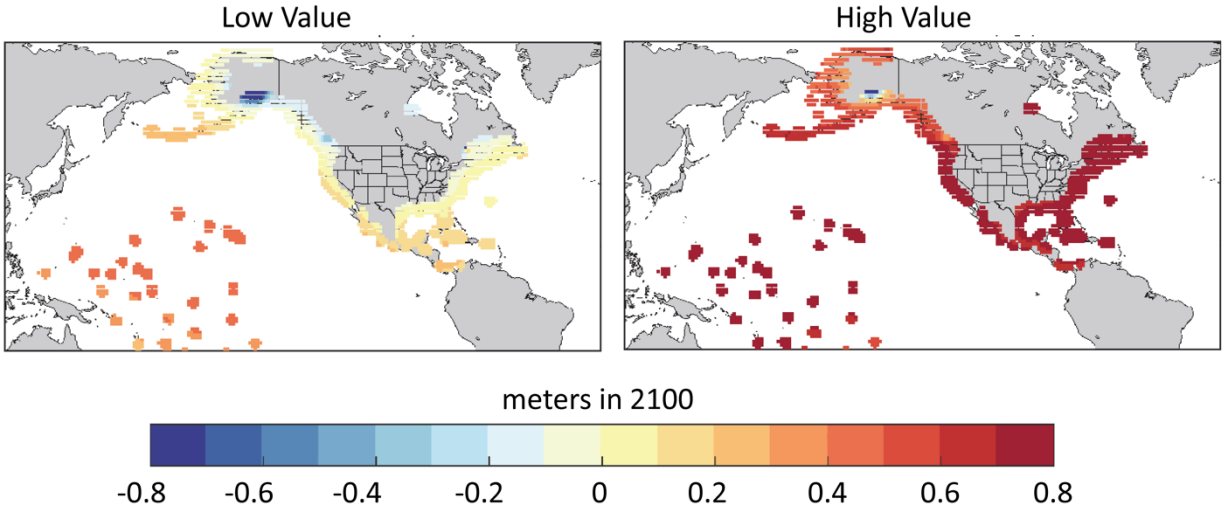

APPENDIX C. LOW AND HIGH TOTAL RSL CHANGE CORRSPONDING TO GMSL SCENARIOS

The maps below show, for each GMSL scenario, a low and high representation of total RSL change in 2100 (relative to 2000) among those samples from the probabilistic RSL distribution consistent with each GMSL scenario. They are presented relative to the median GMSL change for the scenario, as in Figure 9. They are produced by combining the Low scenarios from appendix B with the 17th percentile estimate of background rate, and the High scenarios from appendix B with the 83rd percentile of background rate. They represent an approximate 10th to 90th percentile range.

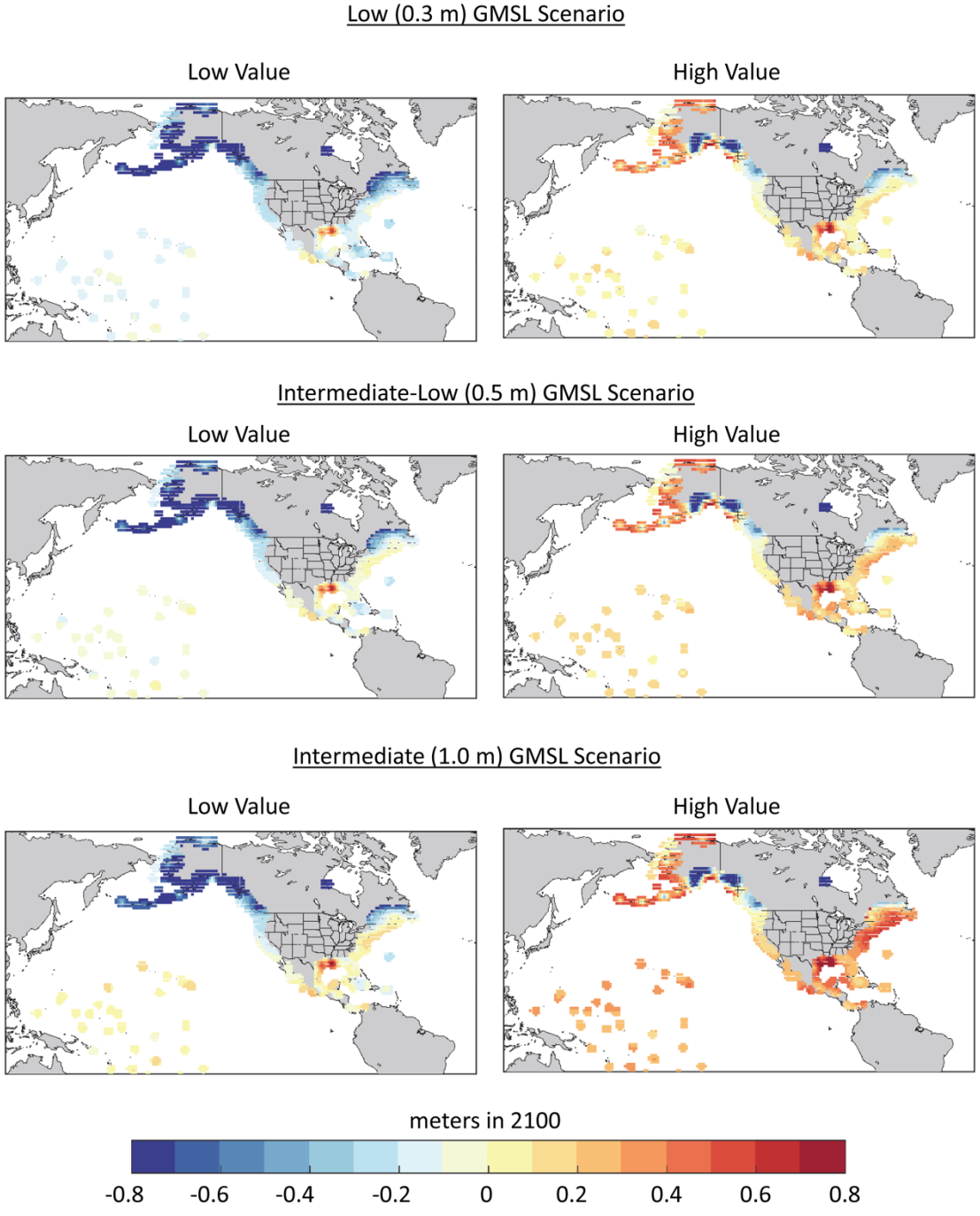

Appendix C: continued

Intermediate-High (1.5 m) GMSL Scenario

Low Value

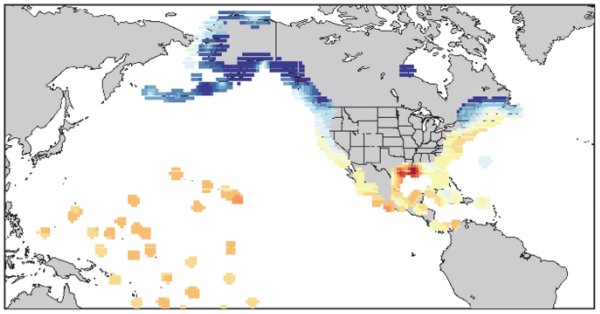

High Value

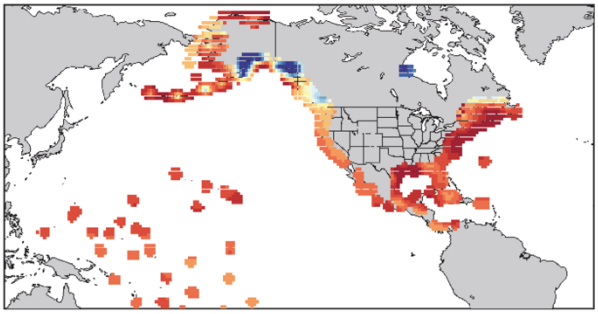

High (2.0 m) GMSL Scenario

Low Value

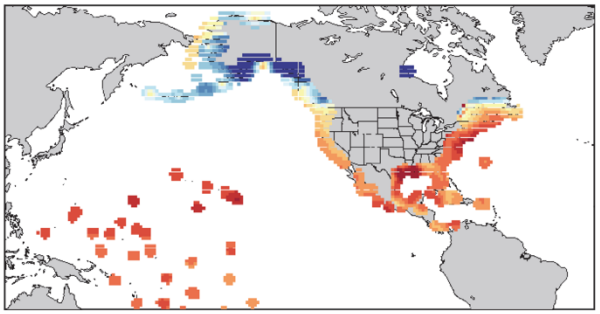

High Value

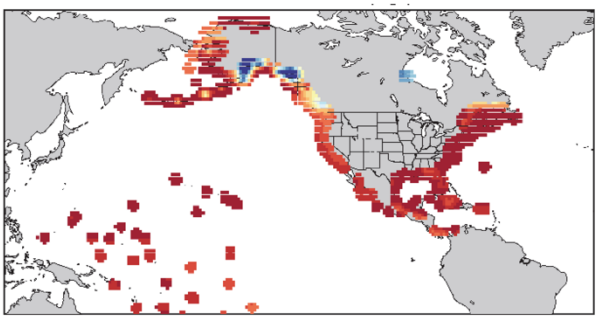

Extreme (2.5 m) GMSL Scenario

Low Value

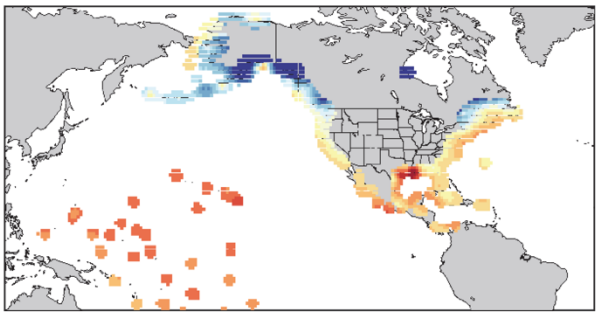

High Value

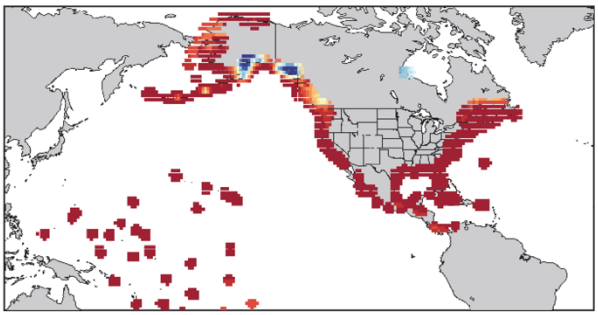

meters in 2100

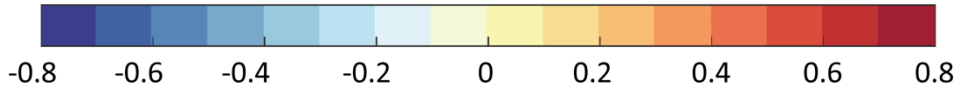

APPENDIX D. CMIP5 MODELS USED

The CMIP5 models indicated in the left set of columns were used for the thermal expansion and ocean dynamics projections in this report. The CMIP5 models indicated in the right set of columns were used as input by Marzeion et al. (2012) to a glacier mass-balance model. The output of this model is a key input for the glacier projections in this report. "21" indicates use for the 21st century projections; "22" indicates the model was also used for 22nd century projections.

Model	Thermal Expansion and Ocean Dynamics			Glaciers and Ice Caps		
	RCP 8.5	RCP 4.5	RCP 2.6	RCP 8.5	RCP 4.5	RCP 2.6
access1-0	21	21				
access1-3	21	21				
bcc-csm1-1	22	22	22	22	22	22
bcc-csm1-1-m	21	21	21			
canesm2	21	22	22	21	22	22
ccsm4	21	21	21	21	21	21
cmcc-cesm	21					
cmcc-cm	21	21				
cmcc-cms	21	21				
cnrm-cm5	22	22	21	22	22	21
csiro-mk3-6-0	21	21	21	22	22	21
gfdl-cm3	21	22	21	21	21	21
gfdl-esm2g	21	21	21			
gfdl-esm2m	21	21	21			
giss-e2-r	22	22	22	22	22	
giss-e2-r-cc	21	21				
hadgem2-cc	21					
hadgem2-es	21		22	22	22	22
inmcm4	21	21		21	21	
ipsl-cm5a-lr	22	22	22	22	22	22
ipsl-cm5a-mr	21	22	21			
miroc-esm	21	22	21	21	21	21
miroc-esm-chem	21	21	21			
miroc5				21	21	21
mpi-esm-lr	22	22	22	22	22	22
mpi-esm-mr	21	21	21			
mri-cgcm3	21		21	21	21	21
noresm1-m	21	22	21	21	22	21
noresm1-me	21	21	21			

ACRONYMS

AR5	Fifth Assessment Report
AIS	Antarctic Ice Sheet
AMO	Atlantic Multidecadal Oscillation
cm	centimeters
CMIP5	Fifth Model Intercomparison Project
CSSR	Climate Science Special Project
DoD	Department of Defense
EAIS	Eastern Antarctic ice sheet
ENSO	El Niño Southern Oscillation
EPA	Environmental Protection Agency
FEMA	Federal Emergency Management Agency
FFRMS	Federal Flood Risk Management Standard
GIA	Glacial isostatic adjustment
GIS	Greenland ice sheet
GCM	Global Circulation Models
GIC	Greenland ice sheet
GMSL	Global mean sea level
GRACE	Gravity Recovery and Climate Experiment
inch	in
IPCC	Intergovernmental Panel on Climate Change
km	kilometer
m	meters
MHHW	Mean higher high water
mm	millimeter
NAO	North Atlantic Oscillation
NASA	National Aeronautics and Space Administration
NCA4	Fourth National Climate Assessment
NESDIS	National Environmental Satellite, Data, and Information Service
NOAA	National Oceanic and Atmospheric Administration
NOC	National Ocean Council
PDO	Pacific Decadal Oscillation
RCP	Representative concentration pathways
RSL	Relative sea level
SSH	Sea surface height
USACE	United States Army Corps of Engineers
USAPI	United States Affiliated Pacific Islands
USGS	United States Geological Survey
USGCRP	United States Global Change Research Program
VLM	Vertical land movement
WAIS	Western Antarctic ice sheet